



**HAL**  
open science

## Modulation of triheteromeric NMDA receptors by N-terminal domain ligands.

Christopher J Hatton, Pierre Paoletti

► **To cite this version:**

Christopher J Hatton, Pierre Paoletti. Modulation of triheteromeric NMDA receptors by N-terminal domain ligands.. *Neuron*, 2005, 46 (2), pp.261-74. 10.1016/j.neuron.2005.03.005 . hal-00139989

**HAL Id: hal-00139989**

**<https://hal.science/hal-00139989>**

Submitted on 4 Apr 2007

**HAL** is a multi-disciplinary open access archive for the deposit and dissemination of scientific research documents, whether they are published or not. The documents may come from teaching and research institutions in France or abroad, or from public or private research centers.

L'archive ouverte pluridisciplinaire **HAL**, est destinée au dépôt et à la diffusion de documents scientifiques de niveau recherche, publiés ou non, émanant des établissements d'enseignement et de recherche français ou étrangers, des laboratoires publics ou privés.

# **Modulation of triheteromeric NMDA receptors by N-terminal domain ligands**

Christopher J. Hatton and Pierre Paoletti

Laboratoire de Neurobiologie  
CNRS UMR 8544  
Ecole Normale Supérieure  
46 rue d'Ulm  
75005, Paris, France

*Running title:* Modulation of triheteromeric NMDA receptors

Correspondence should be addressed to Dr. Pierre Paoletti, Laboratoire de Neurobiologie, Ecole Normale Supérieure, 46 rue d'Ulm, 75005 Paris, France

Tel : 33 1 44 32 38 94 / Fax: 33 1 44 32 38 87 / email: paoletti@biologie.ens.fr

*Key words:* glutamate receptors, NMDA, subunit, modulation, zinc, ifenprodil

*Acknowledgements:* this work was supported by CNRS and Marie Curie fellowships (CJH) and by INSERM (PP). We thank Philippe Ascher, James Kew and Jacques Neyton for comments on the manuscript. We also thank Sanofi-Synthélabo for the gift of ifenprodil.

## SUMMARY

NMDA receptors (NMDARs) are heteromeric assemblies of NR1 and NR2(A-D) subunits whose properties are heavily influenced by the type of NR2 subunit incorporated. While NMDARs containing only one type of NR2 subunit have been extensively characterized, little is known about receptors containing two different NR2 subunits despite compelling evidence that such triheteromeric receptors exist *in vivo*. We have developed a novel point mutation approach which allows isolation of recombinant triheteromeric NMDARs possessing two different NR2 N-terminal domains (NTDs). We show that in receptors associating the NTD of NR2A (sensing nanomolar Zn) and that of NR2B (sensing ifenprodil), each NTD-binding site retains its selective high-affinity for its ligand. However each ligand produces only partial inhibition and occupancy of both NR2-NTDs by their respective ligand is required for maximal inhibition. Similarly, NR1/2A/2C receptors are inhibited by zinc with high potency but low efficacy. Therefore, interactions between homologous N-terminal domains determine the unique pharmacological properties of triheteromeric NMDARs.

## INTRODUCTION

N-methyl-D-aspartate (NMDA) receptors are glutamate-gated ion channels that play critical roles in excitatory neurotransmission, synaptic plasticity and neuronal cell death (Dingledine *et al.*, 1999; Kemp and McKernan, 2002). Early patch-clamp and binding experiments on neurons revealed that native NMDARs do not exist as a single, functionally homogenous, population of receptors but rather as distinct subtypes displaying both regional and developmental variability in their activation/permeation properties. It is now well established that this functional diversity is generated by differential incorporation of various types of subunits (for review see Dingledine *et al.*, 1999; Cull-Candy *et al.*, 2001). NMDARs function as heteromeric assemblies associating NR1 and NR2 subunits, and less commonly NR3 subunits. The NR1 subunit, ubiquitously expressed in the CNS, is encoded by a single gene but occurs as eight distinct isoforms owing to alternative splicing. The NR2 subunits are encoded by four different genes (NR2A to NR2D) and have distinct distributions in the CNS, with patterns of expression that change strikingly during development. In the embryonic brain, NR2B and NR2D subunits predominate, while NR2A and NR2C are absent. In contrast, in the adult brain, NR2A predominates, being ubiquitously expressed, while NR2B expression is restricted to forebrain areas and NR2C is highly enriched in the cerebellum (Watanabe *et al.*, 1992; Ishii *et al.*, 1993; Monyer *et al.*, 1994).

Functional diversity of native NMDARs is usually assumed to result from the existence of four subpopulations of diheteromeric receptors expressing a simple binary combination of NR1 and NR2 subunits. However, as NMDARs are most probably tetramers made of two copies of NR1 and two copies of NR2 (see Schorge and Colquhoun, 2003), functional diversity could also arise from the incorporation of more than one type of NR2 subunit in a same receptor complex. In fact, there is compelling evidence for such heterogeneity in NR2 subunit assembly. Ternary complexes containing NR1/2A/2B have been consistently observed in native tissues, most particularly in the cortex where they represent a sizeable fraction of the NMDA receptor population (Sheng *et al.*, 1994; Didier *et al.*, 1995; Chazot and Stephenson, 1997; Luo *et al.*, 1997). Other ternary complexes associating NR2C or NR2D have also been observed *in vivo*, most particularly NR1/2A/2C complexes in the cerebellum (Chazot *et al.*, 1994; Sundström *et al.*, 1997; Dunah *et al.*, 1998; Cathala *et al.*, 2000; Brickley *et al.*, 2003). While diheteromeric NR1/NR2 receptors have been extensively studied in recombinant systems, the functional attributes of triheteromeric receptors remain largely unknown.

A striking difference between the various diheteromeric NR1/NR2 receptor subtypes is their differential sensitivity to extracellular allosteric modulators, a property that is commonly used to infer the NR2 subunit composition of native NMDARs. Thus, NR1/2A receptors are exquisitely sensitive to Zn ions, being inhibited by low nanomolar concentrations (Williams, 1996; Paoletti *et al.*, 1997; Chen *et al.*, 1997), while NR1/2B receptors are selectively antagonized by ifenprodil, and its derivatives, a class of synthetic compounds with neuroprotectant properties (Williams, 1993). In either case, inhibition occurs through binding of the modulatory ligand (Zn or ifenprodil) to the N-terminal domain (NTD) of the corresponding NR2 subunit (Choi and Lipton, 1999; Fayyazuddin *et al.*, 2000; Low *et al.*, 2000; Paoletti *et al.*, 2000; Perin-Dureau *et al.*, 2002). In this respect, it is unclear whether

triheteromeric receptors associating two different NR2-NTDs are still sensitive to NR2-subunit specific ligands.

The paucity of information regarding the function of triheteromeric receptors results from the fact that expressing, in recombinant systems, more than one type of NR2 subunit yields a mixture of receptor populations (diheteromeric plus triheteromeric receptors) with no easy way to isolate triheteromeric receptors from the co-expressed diheteromeric receptors. We have developed an approach combining mutagenesis and pharmacology, which permits isolation of triheteromeric receptor populations and allows us to study the sensitivity of triheteromeric receptors to subunit-specific extracellular modulators.

## RESULTS

### **NMDARs with only one active high-affinity Zn binding site retain Zn sensitivity**

NR1/2A receptors are thought to be composed of two NR1 and two NR2A subunits and thus contain two high-affinity NR2A-NTD Zn binding sites. We have investigated whether Zn binding to two such sites is a prerequisite for nanomolar Zn sensitivity by investigating the effects of nanomolar concentrations of Zn on NMDARs containing only one active NR2A-NTD Zn binding site.

Co-expression of wild-type (wt) NR1, wt NR2A and a mutant NR2A subunit defective for Zn binding, lead to the expression of three receptor populations. A NR1/2A wt population containing two active NR2A-NTD Zn binding sites, an all-mutant NR1/2A<sub>mutant</sub> population with both NR2A-NTDs mutated, and a triheteromeric NR1/2A/2A<sub>mutant</sub> population, with only one active NR2A-NTD Zn binding site per receptor. In order to study the effect of Zn on the triheteromeric receptor population, we need to be able to selectively eliminate NR1/2A wt receptors, thus leaving triheteromeric receptors as the sole remaining population with active NR2A-NTD Zn binding sites. To this end, we constructed a mutant NR2A subunit containing two point mutations: H128S to prevent nanomolar Zn binding and N614K to prevent external Mg block. H128, located in the NR2A-NTD, is thought to directly participate in Zn coordination and its mutation to serine produces a 520-fold reduction in Zn sensitivity (Fayyazuddin *et al.*, 2000; Paoletti *et al.*, 2000). N614, located at the tip of the M2 loop, is a key determinant of Mg sensitivity and its mutation to positively charged residues abolishes Mg block (Wollmuth *et al.*, 1998 and see Fig. 1B).

*Xenopus* oocytes expressing diheteromeric NR1/2A<sub>H128SN614K</sub> receptors elicited inward currents at -80 mV in response to application of 100  $\mu$ M glutamate and glycine. These currents were almost unaffected ( $4.0 \pm 0.9$  % inhibition, n=8 cells) by application of 1 mM Mg, or by additional application of 200 nM Zn ( $3.9 \pm 0.4$  % inhibition, n=8 cells; Fig. 1B). In contrast, NMDA currents in cells expressing NR1/2A wt receptors were virtually abolished in 1mM Mg (mean  $99.2 \pm 0.3$  % inhibition, n=9 cells; Fig. 1A). Although not evident at -80 mV, additional application of 200 nM Zn also produces a strong inhibition of NR1/2A wt receptors, as revealed in voltage-ramps from -100 to +50 mV (Fig 1A). We confirmed this observation in steady-state recordings in Mg at -30 mV (a potential at which Mg block is not complete), which revealed  $73.1 \pm 1.2$  % (n=3 cells, data not shown) inhibition by Zn (200 nM). Further, NR1/2A<sub>N614K</sub> receptors, which are insensitive to Mg block, showed a similar  $64.2 \pm 3.2$  % (n=4 cells, data not shown) inhibition by 200 nM Zn (in Mg). Thus, the effect of nanomolar Zn on NR1/2A receptors appears to be affected neither by the presence of extracellular Mg, nor by the presence of the N614K mutation.

When the NR2A<sub>H128SN614K</sub> subunit is co-expressed along with both NR1 and NR2A wt subunits, we expect that the oocytes will express three populations of NMDARs. As described above, in 1 mM Mg at -80 mV, the current from NR1/2A wt receptors is almost completely inhibited. Thus, the remaining NMDA receptor current must arise from the Mg-insensitive all-mutant NR1/2A<sub>H128SN614K</sub> receptors, with a possible contribution from triheteromeric NR1/2A/2A<sub>H128SN614K</sub> receptors. When 200 nM Zn was applied under these conditions,  $15.7 \pm 1.5$  % inhibition (n=9 cells) of the whole-cell currents was seen (Fig. 1C). As NR1/2A<sub>H128N614K</sub> receptors are almost unaffected by 200 nM Zn, this

inhibition can only arise from an effect of Zn on the triheteromeric NR1/2A/2A<sub>H128S/N614K</sub> population. Thus, NMDARs possessing only one active NTD Zn binding site retain nanomolar Zn sensitivity.

### **Isolating triheteromeric NMDA receptor populations**

In order to quantify the inhibition by Zn of NMDARs with only one active NTD Zn binding site, we need to be able to functionally isolate a pure triheteromeric NMDA receptor population. The dual point-mutation approach used above permits the elimination of NR1/2A wt receptors with Mg, but does not allow us to separate the contributions from triheteromeric and all-mutant receptors. In order to separate these remaining two populations, we decided to include a further point mutation in our mutant NR2A subunit that altered glutamate sensitivity. By doing so, we should be able to separate triheteromeric and all-mutant receptors on a glutamate concentration-response curve, with all-mutant receptors containing two mutated subunits being further shifted than triheteromeric receptors containing only one mutant subunit (see Laube *et al.*, 1998).

One mutation that appeared interesting for our purposes was a threonine to alanine mutation at position 690 in the glutamate binding site, which induces a shift in the glutamate EC<sub>50</sub> of around 1000-fold without affecting maximum current level (Anson *et al.*, 1998). Further, single-channel analysis revealed that this mutation strongly affects glutamate binding but has very little effect on channel gating (Anson *et al.*, 2000). Structural evidence from the crystallized glutamate binding domain of the AMPA receptor GluR2 support these functional findings, by showing that, T655 (the GluR2 homologue of T690), directly contacts the glutamate molecule through a hydrogen bond with the distal carboxyl group (Armstrong and Gouaux, 2000). As seen by Anson *et al.* (1998), NR1/2A<sub>T690A</sub> receptors produced a large shift in glutamate EC<sub>50</sub> compared to wt (EC<sub>50</sub> = 2.8 ± 0.1 mM vs 4.4 ± 0.2 μM), accompanied by a modest change in Hill slope (n<sub>H</sub> = 1.15 ± 0.02, vs 1.33 ± 0.03, n = 4 vs 9 cells respectively; Fig. 2A left panel). According to Laube *et al.* (1998), the glutamate sensitivity of T690A containing receptors should show different shifts depending on the number of mutant subunits per receptor. Unfortunately, the shift in glutamate sensitivity induced by the T690A mutation was not sufficient to enable us to separate the triheteromeric and all-mutant populations (data not shown).

In an attempt to produce a greater shift in the glutamate EC<sub>50</sub> and hopefully better separate the triheteromeric and all-mutant receptor populations, we introduced three alternative non-polar substitutions at T690, mutating this residue to valine, isoleucine, or leucine. The rationale for such substitutions was to increase side-chain length compared to the initial alanine substitution, hoping to more severely affect glutamate binding. The resulting glutamate concentration-response curves for NR1/2A<sub>T690V</sub>, 2A<sub>T690L</sub> and 2A<sub>T690I</sub> receptors are shown in Fig. 2. While the T690V mutation, induced a slightly smaller shift in glutamate sensitivity than T690A (EC<sub>50</sub> 1.1 ± 0.02 mM, n<sub>H</sub> = 1.26 ± 0.01, n = 10), the T690I or T690L mutations produced huge shifts in glutamate EC<sub>50</sub>. At 24h after injection, which is sufficient for expression of large-currents in cells expressing NR1/2A wt or the T690A or T690V mutant receptors (0.5-5 μA), whole-oocyte currents from cells expressing NR1/2A<sub>T690I</sub> or NR1/2A<sub>T690L</sub> receptors in response to 10 mM glutamate (plus 100 μM glycine) were only of the order of 10-20 nA. Only after 72h, was expression sufficient (maximal currents at 10 mM glutamate of several hundred nA) to permit estimation of the lower part of the glutamate concentration-response

curve. Whilst it is impossible to provide accurate glutamate  $EC_{50}$ s for these two mutations, as we only have the very foot of the glutamate concentration-response curve, they are most probably in the molar range, with estimations  $>10$  M ( $n_H$  fixed=1,  $n=3$  each). Despite the risk that the T690I or T690L mutant subunits could act in a negative dominant manner when incorporated into triheteromeric receptors, we combined T690I with the N614K and H128S mutations. The resulting NR1/2A<sub>N614KT690I</sub> and NR1/2A<sub>H128SN614KT690I</sub> receptors showed glutamate sensitivities that were similar to the NR1/2A<sub>T690I</sub> receptors ( $n=5$  each, Fig. 2B), indicating that the inclusion of the Zn and Mg binding mutations did not interfere with the glutamate binding.

When the NR2A<sub>H128SN614KT690I</sub> subunit was subsequently co-expressed with wt NR1 and NR2A subunits, the resulting glutamate concentration-response curves in zero Mg (24h after injection) showed only two components, with  $EC_{50}$ s of  $4.1 \pm 0.1$   $\mu$ M and  $3.0 \pm 1.3$  mM (relative areas  $72 \pm 3$  % and  $28 \pm 6$  %,  $n_H = 1.19 \pm 0.09$  and  $1.27 \pm 0.67$ ,  $n=6$ , Fig. 3). This is to be expected if the contribution to whole-oocyte currents from the all-mutant NR1/2A<sub>H128SN614KT690I</sub> receptors is negligible. Indeed, in parallel experiments with cells injected only with NR1 and NR2A<sub>H128SN614KT690I</sub> subunits, currents were over 100-fold smaller (at 24h) than those from cells expressing all three subunit types, indicating that the likely contribution to whole-oocyte currents from the all-mutant NR1/2A<sub>H128SN614KT690I</sub> receptors is less than 1%. As expected repeating the glutamate concentration-response curves in 1 mM Mg, virtually abolished the high-affinity (NR1/2A wt) component, leaving an almost pure triheteromeric receptor population with an  $EC_{50}$  corresponding to that of the low-affinity component in the absence of Mg ( $EC_{50}$   $4.0 \pm 0.8$  mM, relative area  $98 \pm 5$  %,  $n_H = 0.86 \pm 0.06$ ,  $n = 6$ ).

Exactly the same principle was used to isolate NR1/2A<sub>N614KT690I</sub>/2B or NR1/2A<sub>N614KT690I</sub>/2C receptors following co-injection of NR1, NR2A<sub>N614KT690I</sub> and NR2B or NR2C cDNAs (see supplementary Fig. 1). However, we could not entirely suppress the contribution to whole-oocyte currents from NR1/2C wt receptors with Mg. NMDARs containing the NR2C subunit are known to be less sensitive to Mg block than NR2A or NR2B containing receptors (see Dingledine *et al.*, 1999). In our hands, the NR1/2C component was  $93.9 \pm 0.2$  % ( $n=3$ , data not shown) inhibited by 1 mM Mg at -80 mV, but nonetheless still accounted for  $\sim 14$  % of the residual whole-oocyte currents in Mg (supplementary Fig. 1). Increasing external Mg concentration to 3 mM and/or hyperpolarizing cells to -100 mV, did not significantly increase block ( $n=3$ , data not shown).

### **Quantification of Zn inhibition of NR1/2A NMDARs with only one active NTD Zn binding site**

As described above, after co-injection of wt NR1 and NR2A cDNAs along with the NR2A<sub>H128SN614KT690I</sub> cDNA, a pure triheteromeric NR1/2A/2A<sub>H128SN614KT690I</sub> receptor population with only one active NR2A-NTD Zn binding site per receptor can be isolated by recording currents in 10 mM glutamate, 100  $\mu$ M glycine and 1 mM Mg at -80 mV. Under these conditions, triheteromeric NR1/2A/2A<sub>H128SN614KT690I</sub> receptors were inhibited by Zn in a concentration-dependent manner. Notably, inhibition was evident even at low nanomolar concentrations (Fig. 4A). The Zn inhibition curve was biphasic, with a first high-affinity component in the nanomolar concentration range ( $IC_{50}$   $28.6 \pm 8.1$  nM), much like NR1/2A wt or Mg-insensitive NR1/2A<sub>N614K</sub> receptors ( $IC_{50}$ s  $17.6 \pm 0.6$  nM and  $14.5 \pm 2.3$  nM respectively) presumably reflecting binding to the remaining NR2A-NTD Zn binding site. The second lower affinity

component shows a similar affinity to that of all mutant NR1/2A<sub>H128SN614K</sub> receptors which possess two mutant NTD binding sites ( $IC_{50}$ s  $5.0 \pm 0.9 \mu\text{M}$  vs  $9.0 \pm 1.0 \mu\text{M}$ ) or to that of NR2A-NTD-deleted receptors ( $IC_{50} \sim 12 \mu\text{M}$ ; Rachline *et al.*, 2005). This low-affinity component can be accounted for by Zn binding to a non-NTD binding site common to all NMDA receptor subtypes (Rachline *et al.*, 2005). Strikingly, the degree of inhibition associated with the first component is much reduced compared to NR1/2A wt or NR1/2A<sub>N614K</sub> receptors. As shown in Fig. 4B, in triheteromeric receptors, this high-affinity component of Zn inhibition plateaus at  $14.1 \pm 0.2 \%$  inhibition, compared to  $80.4 \pm 0.1 \%$  for NR1/2A wt receptors ( $66.5 \pm 4 \%$  for NR1/2A<sub>N614K</sub>). Thus although Zn still binds to triheteromeric receptors with high-affinity, the efficacy of inhibition by nanomolar Zn appears much reduced when only one active NR2A-NTD Zn binding site is present (see Discussion).

We were concerned that the inclusion of the glutamate binding site mutation might interfere with NR2-NTD function. Consequently, we repeated Zn inhibition curves in Mg on cells expressing NR1, NR2A and NR2A<sub>H128SN614K</sub> subunits (no glutamate mutation, see Fig. 1C). This approach was justified by parallel experiments which indicated that all-mutant NR1/2A<sub>H128SN614K</sub> receptors yield currents approximately 20-fold smaller than NR1/2A wt (probably due to a reduced single-channel conductance; see Béhé *et al.*, 1995). Thus, we believe that, in Mg, the contamination from all-mutant NR1/2A<sub>H128SN614K</sub> receptors is less than 10%, so the majority of the current is carried by triheteromeric NR1/2A/2A<sub>H128SN614K</sub> receptors. The resulting Zn inhibition profile was strikingly similar to that obtained on NR1/2A/2A<sub>H128SN614KT690I</sub> receptors (see supplementary Fig. 2), demonstrating that the inclusion of the T690I mutation has little effect on Zn inhibition at the NR2A-NTD.

### Zn sensitivity of triheteromeric NR1/2A/2C NMDARs

Biochemical and pharmacological evidence supports the idea that NMDARs composed of NR1, NR2A and NR2C subunits can co-assemble into triheteromeric complexes and are present in mature cerebellum (Wafford *et al.*, 1993; Chazot *et al.*, 1994; Cathala *et al.*, 2000). What the functional and modulatory properties of such receptors may be remains to be determined. From the point of view of Zn modulation, this combination is potentially interesting: whilst the NTD of the NR2A receptor constitutes a nanomolar affinity Zn binding site, the NTD of the NR2C subunit does not bind Zn (Rachline *et al.*, 2005). In order to assess the possible Zn sensitivity of triheteromeric NR1/2A/2C receptors, we co-expressed NR1, NR2C and NR2A<sub>N614KT690I</sub> subunits in *Xenopus* oocytes. The resulting triheteromeric NR1/2A<sub>N614KT690I</sub>/2C receptor population was then functionally isolated within the limits stated above (supplementary Fig. 1).

As for NR1/2A/2A<sub>H128SN614KT690I</sub> receptors, NR1/2A<sub>N614KT690I</sub>/2C receptor currents showed concentration-dependent Zn inhibition, with inhibition evident even in the low nanomolar range, a range where NR1/2C receptors are unaffected (Fig. 5A). The Zn inhibition curve was biphasic, with an  $IC_{50}$  for the high-affinity component of  $5.6 \pm 3.8 \text{ nM}$  and a plateau at  $28.7 \pm 5.0 \%$  (Fig. 5B). Thus, in common with NR1/2A/2A<sub>H128SN614KT690I</sub> receptors which similarly possess only one active NR2A-NTD Zn binding site, triheteromeric NR1/2A<sub>N614KT690I</sub>/2C receptors retain nanomolar Zn sensitivity, but the efficacy of Zn inhibition is much reduced in this concentration range compared to receptors with two NR2A-NTD Zn binding sites.

### Zn and ifenprodil sensitivity of triheteromeric NR1/2A/2B NMDARs

There is compelling biochemical evidence suggesting that NR1/2A/2B triheteromeric receptors are present *in vivo* in forebrain neurons (Sheng *et al.*, 1994; Didier *et al.*, 1995; Chazot and Stephenson, 1997; Luo *et al.*, 1997). This raises the possibility that there exists *in vivo* a population of Zn (nanomolar) and ifenprodil sensitive NMDARs. Consequently, we expressed NR1, NR2B and NR2A<sub>N614KT690I</sub> subunits in *Xenopus* oocytes in order to investigate the modulatory properties of such receptors. As with the other triheteromeric receptors, NR1/2A<sub>N614KT690I</sub>/2B receptors were isolated pharmacologically on the basis of their Mg and glutamate sensitivities so that modulation of their function by NTD ligands could be investigated (see supplementary Fig. 1).

Triheteromeric NR1/2A<sub>N614KT690I</sub>/2B receptor currents were inhibited in a concentration-dependent manner by extracellular Zn (Fig. 6A). However, the Zn inhibition curve, unlike those described above was almost equally well fit by either a 2 or 3 component Hill equation. The highest affinity component of the Zn inhibition curve consistently gave an IC<sub>50</sub> of around 15 nM, regardless of the assumptions of the fit, showing a similar affinity to that of NR1/2A wt, NR1/2A/2A<sub>H128SN614KT690I</sub> and NR1/2A<sub>N614KT690I</sub>/2C receptors suggesting that it reflected Zn binding to the NTD of the NR2A subunit. As with other triheteromeric receptors, the degree of inhibition associated with this high-affinity component (17-38% depending on the assumptions of the fit) was reduced compared to NR1/2A wt receptors, but it was similar to that seen with other triheteromeric receptors containing only one active NR2A-NTD Zn binding site. The second intermediate-affinity Zn binding site was less well defined, but showed a similar affinity to that of NR1/2B wt receptors (0.83 ± 0.28 μM in 3 component fits or 0.78 ± 0.17 μM in 2 component fits vs 0.84 ± 0.03 μM for wt). This most probably reflects Zn binding to the sub-micromolar affinity Zn binding site located on the NR2B-NTD (Rachline *et al.*, 2005). It should also be noted that in two component fits the Hill slope of the second component was very shallow (n<sub>H</sub> = 0.6 ± 0.05) indicative of a fit to a mixed population of binding sites, suggesting that there are in fact three different Zn binding sites with different affinities in NR1/2A<sub>N614KT690I</sub>/2B receptors. The fact that these curves could be fit by two or three component Hill equations probably reflects the difficulty in separating the sub-micromolar NR2B-NTD Zn binding site from the low micromolar non-NR2-NTD Zn binding site common to all NMDA receptor subtypes, which have only a 15-fold difference in affinity (Rachline *et al.*, 2005).

Since NR1/2A<sub>N614KT690I</sub>/2B receptors contain an ifenprodil binding site, located on the NTD of the NR2B subunit (Perin-Dureau *et al.*, 2002), they should be ifenprodil as well as Zn sensitive. Indeed, application of ifenprodil produced a concentration-dependent inhibition of such receptors (Fig. 6B). In the sub-micromolar range, where NR1/2A<sub>N614K</sub> receptors are unaffected (IC<sub>50</sub> 487 ± 24 μM), NR1/2A<sub>N614KT690I</sub>/2B receptors showed a high-affinity for ifenprodil (IC<sub>50</sub> 0.80 ± 0.17 μM), similar to that of NR1/2B wt receptors (IC<sub>50</sub> 142 ± 8 nM, Fig. 6B). However, the ifenprodil inhibition of triheteromeric receptors was biphasic, the high-affinity component having a plateau at 20.6 ± 1.1% compared to 94.2 ± 1.9 % for NR1/2B wt receptors. Thus, as was seen for Zn inhibition, it appears that receptors with only one NR2B-NTD binding site for ifenprodil show a modest change in IC<sub>50</sub>, but a large change in the extent of inhibition.

### **Inhibition of triheteromeric NR1/2A/2B receptors by ifenprodil and Zn is superadditive**

The observation that triheteromeric receptors which possess only one binding site for a particular NTD ligand retain high-affinity but with a low efficacy of inhibition raises the possibility that when (nanomolar) Zn and ifenprodil are applied together to NR1/2A<sub>N614KT690I</sub>/2B receptors, occupation of the two available NR2 NTD sites (Zn on the NR2A<sub>N614KT690I</sub> subunit, ifenprodil on the NR2B subunit), will lead to restoration of high-efficacy inhibition. Fig. 6C shows an example of just such an experiment. When 3  $\mu$ M ifenprodil is applied in a background of 100 nM Zn, the observed inhibition caused by ifenprodil is doubled ( $36.7 \pm 2.5\%$  of the residual current) compared to the inhibition observed when ifenprodil is applied alone ( $18.5 \pm 0.4\%$ ). The same is true if 100 nM Zn is applied in the presence of 3  $\mu$ M ifenprodil ( $48 \pm 1.8\%$  inhibition compared to  $27.7 \pm 0.8\%$ , data not shown). The average results from 4 cells are shown in Fig 6C (right). Similar results were obtained for a range of Zn and ifenprodil concentrations (20-100 nM and 1-3  $\mu$ M respectively; data not shown). Thus it appears that when both NR2-NTDs are occupied the efficacy of inhibition is increased. One interesting point of note is that although these effects are superadditive, the combined inhibition in the presence of both Zn and ifenprodil is only around 55% inhibition. At the same concentrations we would expect  $\sim 70\%$  inhibition of NR1/2A receptors by Zn or  $\sim 95\%$  inhibition of NR1/2B receptors by ifenprodil. Whilst the concentrations used are not quite saturating (they were chosen to be specific for their respective binding sites), this result does suggest that the maximal inhibition, when both NTDs are occupied, is not as marked for NR1/2A/2B receptors as for NR1/2A or NR1/2B receptors.

### **Distinct macroscopic kinetics of ifenprodil inhibition on triheteromeric and wild-type receptors**

We took advantage of the fact that the macroscopic kinetics of ifenprodil inhibition on NR2B containing NMDARs are sufficiently slow ( $\tau_{\text{off}} \sim 1$  min) that they can be assessed in whole-oocyte recordings (Williams, 1993; Perin-Dureau *et al.*, 2002). We therefore compared the kinetics of ifenprodil inhibition on NR1/2B wt and NR1/2A<sub>N614KT690I</sub>/2B triheteromeric receptors. Fig. 7A shows typical responses of NR1/2B and NR1/2A<sub>N614KT690I</sub>/2B receptors to 3  $\mu$ M ifenprodil. Not only are triheteromeric receptors inhibited to a much lesser extent than diheteromeric NR1/2B receptors, but when the inhibitions are normalized it becomes evident that the kinetics of inhibition and not just the extent change. The macroscopic on rate is slower in the triheteromeric receptors, whilst wash out is more rapid (Fig. 7B/C). On average the  $\tau_{\text{on}}$  was doubled from  $3.9 \pm 0.3$  s ( $n=7$ ) in NR1/2B wt to  $8.9 \pm 0.7$  s ( $n=11$ ) in triheteromeric NR1/2A<sub>N614KT690I</sub>/2B receptors, whilst the macroscopic off rate ( $\tau_{\text{off}}$ ) was slightly more than halved from  $78 \pm 8$  s ( $n=4$ ) for NR1/2B, to  $29 \pm 5$  s ( $n=8$ ) for triheteromeric receptors. The fact that the macroscopic kinetics of ifenprodil inhibition are distinct for NR1/2A/2B and NR1/2B receptors is not unexpected since the triheteromeric receptors only contain one ifenprodil binding site, whilst the diheteromers possess two. That  $\tau_{\text{on}}$  is slower and  $\tau_{\text{off}}$  is faster may reflect differences in the affinity of the binding site on the NR2B subunit when paired with an NR2A subunit; it may also reflect the change in efficacy of singly-liganded vs doubly-liganded closures of NTDs (see Discussion). Regardless of the underlying mechanism, these results reveal that the macroscopic kinetics of ifenprodil inhibition reflect NR2B subunit copy number.

## DISCUSSION

By using a novel approach based on a combination of point mutations, we have been able to functionally isolate recombinant NMDA receptors containing NR1 and two different NR2 subunits (triheteromeric receptors). This allowed us to establish the functional stoichiometry of high-affinity Zn inhibition at NR1/2A receptors and to define the sensitivity of triheteromeric NMDA receptors to allosteric modulators binding to the NR2-NTDs. We have unmasked a general rule for NTD function, which is that triheteromeric assemblies including only one ligand-binding NR2-NTD suffices to confer high-sensitivity to its ligand, be it Zn or ifenprodil. Such assemblies, however, show a greatly reduced degree of inhibition compared to their diheteromeric counterparts containing two copies of the same NR2-NTD. High-efficacy inhibition, as seen on NR1/2A and NR1/2B receptors, requires occupancy of both available NR2-NTDs by their respective ligands, a principle applicable even to receptors containing two different NR2 subunits.

One potential problem of our approach is that it was necessary to introduce a strong glutamate binding mutation into the NR2A subunit to isolate the triheteromeric receptor assemblies. Because little is known about the nature of interactions between the NTDs and the agonist binding domains, the possibility exists that NTD ligands could act differently on our mutated triheteromeric receptors than on native triheteromeric NMDARs. We believe that this is not the case for the following reasons. Firstly, on NR1/2A<sub>N164KT690I</sub>/2B receptors, the super-additivity experiments demonstrate that both NR2-NTDs are functional despite the presence of the glutamate mutation. Secondly, either Zn or ifenprodil can inhibit these receptors with similar plateaus although the Zn binds to the glutamate mutated subunit, whereas ifenprodil binds to a wt subunit. Thirdly, and most importantly, we have obtained direct experimental evidence that NR2-NTD function is not affected by the presence of the glutamate binding mutation by recording from cells expressing NR1, NR2A and NR2A<sub>H128SN614K</sub> subunits under conditions of minimal contamination by all-mutant receptors (see supplementary Fig. 2). Zn concentration-inhibition curves in these cells are almost identical to those recorded from NR1/2A/2A<sub>H128SN614KT690I</sub> receptors. Together, these findings indicate that the T690I-mutation does not affect the ability of NTD-ligands to inhibit NMDARs, suggesting that our current findings are directly applicable to native triheteromeric assemblies.

The discovery that triheteromeric NR1/2A/2B receptors are inhibited by ifenprodil with high-affinity but only to a limited degree, might explain the apparent controversy surrounding the ifenprodil sensitivity of NR1/2A/2B receptors. Kew *et al.* (1998) suggested that ifenprodil sensitive NR1/2A/2B receptors were present in cultured cortical neurons, but Tovar and Westbrook (1999) argued against this because they saw only limited ifenprodil inhibition in HEK-293 cells co-expressing NR1, NR2A and NR2B subunits. Interpretation of the findings in either case is complicated by the fact that they are based on results from cells expressing mixtures of di- and tri-heteromeric receptors. Using a direct biochemical approach, Hawkins *et al.* (1999) found that in HEK-293 cells transfected with the NR1, NR2A and NR2B subunits, receptors purified with an anti-NR2A antibody showed significant high-affinity binding to the ifenprodil derivative [<sup>3</sup>H]Ro 25-6981, implying that NR1/2A/2B receptors bind ifenprodil and its derivatives with high-affinity, as suggested by Kew *et al.* (1998), but apparently at

odds with the observation of Tovar and Westbrook (1999). Our present observation that NR1/2A<sub>N614KT690I</sub>/2B receptors have a high-affinity for ifenprodil but are inhibited to only a limited extent ties together these apparently divergent observations. Further, our finding that macroscopic on- and off-rates of ifenprodil inhibition on these receptors differ from those on NR1/2B wt receptors, may now serve as a useful tool for detecting the presence of triheteromeric NR1/2A/2B receptors *in vivo*.

The NR2-NTDs are structurally related to the bacterial protein LIVBP (leucine/isoleucine/valine binding protein) and to other LIVBP-like domains found in other membrane receptors, in particular the agonist-binding domains (ABDs) of metabotropic glutamate and GABA receptors (Paoletti *et al.*, 2000; Pin *et al.*, 2003). Functional and crystallographic studies of a number of LIVBP-like domains have revealed that these domains fold as two lobes separated by a central cleft and that they oscillate between an “open” and “closed” cleft conformations, the later being stabilized upon ligand binding within the cleft (“Venus-flytrap” mechanism; see Pin *et al.*, 2003). Both Zn and ifenprodil act via binding sites located in the cleft of their respective NR2-NTDs and have been proposed to promote cleft closure (Paoletti *et al.*, 2000; Perin-Dureau *et al.*, 2002). In other words, Zn and ifenprodil can be considered as *agonists* of their respective NTD-binding sites, the activation of which leads to inhibition of the receptor. Exactly how activation (closure) of the NTD-domains leads to inhibition of the receptor is still poorly understood. One suggestion is that binding of Zn or ifenprodil to the NR2-NTDs induces a shift of the proton sensitivity rendering the receptors more sensitive to inhibition by ambient protons (Mott *et al.*, 1998; Low *et al.*, 2000). In Fig. 8, we show two possible NTD activation mechanisms which could account for NR2-NTD inhibition of NMDARs. They are based on our knowledge of the stoichiometry of NMDARs (two NR1 and two NR2 subunits) and on our present results. We know that there are two potential NR2-NTD binding sites per receptor, and that both singly- and doubly-NTD-liganded states can lead to inhibition, but that the degree of inhibition of the doubly-NTD-liganded receptors is greater (higher efficacy) than that of singly-NTD-liganded receptors. What we do not know is whether, the NR2-NTDs move in a concerted fashion (scheme 1) or independently (scheme 2).

In the first case, we assume that the NR2-NTDs can only change conformation in a concerted manner, being either both open or both closed. The difference in efficacy of inhibition between singly- and doubly-NTD-liganded states results from the fact that the stability of the doubly-NTD-liganded closed state is greater than the singly-NTD-liganded closed state (efficacy  $E_2 = \beta_2/\alpha_2 > E_1 = \beta_1/\alpha_1$ ). In the second case, where the NR2-NTDs can move independently from one another, inhibition can arise from receptors with either one or both NR2-NTDs closed. In this scenario, receptors with one open NR2-NTD and one closed NR2-NTD have only partial access to the downstream inhibitory machinery, and only receptors with both NR2-NTDs closed have full access (potentially by partial or full unmasking of a proton sensor). Importantly, in this scheme, singly-NTD-liganded receptors give access only to the state with partial access to the downstream inhibitory machinery whereas doubly-NTD-liganded receptors give access to both singly- and doubly-NTD-shut states, with partial or full access to the inhibitory machinery.

Using parameters chosen to give the correct  $IC_{50}$  for the wt receptors (18 nM), and correct relative inhibitions for wt and triheteromeric receptors, the schemes shown in Fig. 8A result in the

predicted concentration-inhibition curves and Hill slope-concentration curves shown in Fig. 8B/C. Both models predict Zn  $IC_{50}$ s for the triheteromeric receptors in the low nanomolar range as experimentally observed. Scheme 1 predicts the correct tendency with regards to the relative  $IC_{50}$ s of wt and triheteromeric receptors, with an  $IC_{50}$  of 25 nM for triheteromeric receptors with only one active NR2-NTD (red curves), very close to the experimentally determined value for NR1/2A/2A<sub>H128SN614KT690I</sub> receptors (29 nM). Scheme 2 in contrast, predicts an  $IC_{50}$  of 10 nM (red curves), a shift in the wrong direction. However, scheme 2 gives a much better prediction than scheme 1 of the shallow Hill-slopes, characteristic of high-affinity Zn and ifenprodil inhibitions of wt NMDARs (Paoletti *et al.*, 1997; Chen *et al.*, 1997; Kew *et al.*, 1998; Masuko *et al.*, 1999; Perin-Dureau *et al.*, 2002). Scheme 2 predicts a Hill slope of 1.07, very close to the experimentally determined value (1.06), whilst scheme 1 predicts a steeper slope of 1.33 (see Fig. 4 and green curves, Fig. 8). The shallow Hill-slopes can at first seem at odds with the presence of two potential binding sites per receptor (two NR2 subunits). Our findings now provide an explanation for this, as both our models predict a shallowing of the concentration-inhibition curve when singly-liganded inhibition is taken into account (green vs blue lines). Interestingly, a precedent in favour of scheme 2 comes from dimeric metabotropic glutamate receptors (mGluRs) which possess ABDs structurally related to the NTDs of NMDARs. Indeed, Kniazeff *et al.* (2004) found that in mGluRs, binding of agonist to both ABDs is required for full activity, but that partial activity can be observed when one ABD is occupied by glutamate while the other is blocked open by an antagonist. For NMDARs, further investigation will be needed to differentiate between the two models.

One interesting observation made during the course of this study was that, whilst the  $IC_{50}$  for Zn inhibition of the NR1/2A/2A<sub>H128SN614KT690I</sub> receptors was very similar to that of NR1/2A wt receptors, the glutamate  $EC_{50}$  of these triheteromeric receptors was, by contrast, very different from that of either NR1/2A wt or all-mutant NR1/2A<sub>H128SN614KT690I</sub> receptors. This suggests that the nature of the interactions between the glutamate binding sites of the NR2A subunits is very different from the interactions of their NTDs, despite the fact that the two domains share similar bi-lobate folds and Venus-flytrap mechanism (Mayer and Armstrong, 2004). At the level of the agonist binding sites, it is known that NMDA receptor gating has an absolute requirement for the binding of two molecules of glutamate and two molecules of glycine (Benveniste and Mayer, 1991; Clements and Westbrook, 1991). Again, this is fundamentally different from the effects of inhibitory agonists of the NR2-NTD where one agonist molecule is sufficient to produce partial inhibition (see above). Since all the agonist binding sites need to be occupied for the channel to open, introducing one subunit with a mutation which causes a very large shift in glutamate sensitivity, such as T690I, might prevent channel activation. That T690I-containing NR2A subunits did not act in a negative dominant manner (see Fig. 3) provides new information about the nature of the interactions between glutamate binding sites. It suggests a strong cooperativity between the two glutamate binding sites, such that the site of the T690I containing subunit increases in affinity when the site of the wt subunit is occupied. We cannot say how this cooperativity arises, but a likely explanation for this phenomenon is a direct physical interaction from one glutamate binding domain to the other. This seems a particularly attractive hypothesis, since isolated glutamate binding domains of AMPA GluR2 subunits form dimers (Sun *et*

*et al.*, 2002) and since NR1 glycine binding domains have also been suggested to form homodimers (Neugebauer *et al.*, 2003; but see also Furukawa and Gouaux, 2003). Thus, despite the fact that NTDs fold similarly to the ABDs and also dimerize (Kuusinen *et al.*, 1999; Ayalon and Stern-Bach, 2001; Meddows *et al.*, 2001), NTDs and the ABDs appear to function differently. This could reflect differences in domain-domain interaction, as the interface seen in dimeric GluR2 ABDs (Sun *et al.*, 2002) differs from that seen in dimeric mGluR ABDs (Kunishima *et al.*, 2000) which are structurally related to the NTD of ionotropic glutamate receptors. Alternatively, this could indicate differences in quaternary arrangement, with homodimers, NR1-NR1, NR2-NR2, formed at the level of the ABDs but heterodimers, NR1-NR2 formed at the level of the NTDs.

The presence of NR1/2A/2B receptors in adult forebrain neurons was demonstrated as early as 1994 (Sheng *et al.*, 1994; see also Didier *et al.*, 1995; Chazot and Stephenson, 1997; Luo *et al.*, 1997), yet little is known of their functional properties. Similarly, there is increasing evidence that triheteromeric NR1/2A/2C receptors are present in the adult cerebellum (Wafford *et al.*, 1993, Chazot *et al.*, 1994; Cathala *et al.*, 2000). There is also accumulating evidence that Zn<sup>2+</sup> ions, which are stored and released at many glutamatergic synapses in the brain, are important endogenous regulators of NMDA receptor activity (Smart *et al.*, 2004). Basal Zn levels are thought to provide tonic inhibition of NMDARs by binding at high-affinity (nanomolar) Zn binding sites, while synaptically released Zn could provide phasic inhibition of NMDARs by binding at sites of lower (micromolar) affinity (see Rachline *et al.*, 2005). We now demonstrate that both NR1/2A/2B and NR1/2A/2C receptors retain NR1/2A-like nanomolar Zn sensitivity. This suggests that NR2A-containing triheteromeric NMDARs, similarly to NR1/2A receptors, may also be subject to tonic inhibition at physiological concentrations of ambient Zn. However, because the degree of inhibition is reduced compared to diheteromeric NR1/2A receptors, the regulation of NR2A subunit expression relative to that of NR2B or NR2C subunits might provide a way by which cells can fine tune background NMDA receptor activity as a function of ambient Zn concentration. Another striking feature of NR1/2A/2B receptors, is their graded inhibition over a range of Zn concentrations, spanning almost three orders of magnitude, from the nanomolar to micromolar range. So, unlike NR1/2A receptors, which are strongly inhibited by tonic (nanomolar) Zn levels, and NR1/2B receptors, which only sense phasic (micromolar) Zn (Rachline *et al.*, 2005), triheteromeric NR1/2A/2B receptors could sense both tonic and phasic Zn. Finally, we find that triheteromeric NR1/2A/2B receptors retain high-affinity ifenprodil sensitivity but that the degree of inhibition strongly depends on the occupancy of the neighbouring NR2A NTD high-affinity Zn binding site and thus on ambient Zn levels. Since ifenprodil is the prototype compound of a family of NR2B-specific antagonists with promising neuroprotective properties (Kemp and McKernan, 2002), this finding could have important implications for the effects of ifenprodil-like compounds *in vivo* and their therapeutic potentials.

## Experimental Procedures

*Molecular biology.* The expression plasmids (for rat NR1-1a, rat NR2A, mouse  $\epsilon 2$  [referred to hereafter as NR2B] and rat NR2C), the mutagenesis strategy and sequencing are as previously described in Paoletti *et al.* (1997) and Rachline *et al.* (2005).

*Electrophysiology and solutions.* *Xenopus laevis* oocytes were isolated, maintained, injected, voltage-clamped and superfused as described by Paoletti *et al.* (1997). Oocytes were injected with 30-40 nl of mixtures of wt NR1, wt NR2 and mutant NR2 cDNAs (10 ng/ $\mu$ l) in the ratio of 1:2, NR1:NR2 respectively, for diheteromeric receptors and of 1:1:2 for triheteromeric NR1/2A/2A<sub>mutant</sub> and NR1/2B/2A<sub>mutant</sub> receptors. For NR1/2C/2A<sub>mutant</sub> triheteromeric receptors, a ratio of 1:2:1 was injected to counter-balance the lower expression rate for the NR2C subunit compared to the NR2A subunit. Currents were recorded after 1-3 d expression, with a Warner Instruments OC-725 amplifier, filtered at 40 Hz and data sampled at 250 Hz with pClamp 7.0 (Axon Instruments). All experiments were performed at room temperature (20-24°C).

The control solution for superfusion contained (in mM): 100 NaCl, 5 HEPES, 0.3 BaCl<sub>2</sub>, and 10 tricine (N-tris[hydroxymethyl]methylglycine, used to chelate trace amounts of contaminating Zn; Paoletti *et al.*, 1997), pH was adjusted to 7.3 with KOH. Glycine and L-glutamate were prepared as 100 mM or 1M aliquots in bidistilled water and stored at -20°C. In all experiments glycine was applied at 100  $\mu$ M. For applications of 30 mM glutamate containing solutions, Na-L-glutamate was dissolved directly in the control solution and pH readjusted accordingly. Ifenprodil (a gift from B. Scatton, Sanofi-Sythelabo) was prepared in 50  $\mu$ l aliquots in bidistilled water at 10 mM and stored at -20°C. ZnCl<sub>2</sub> stock solutions (100  $\mu$ M – 100 mM) were prepared by serial dilutions in bidistilled water from an initial stock at 100 mM dissolved in 10<sup>-2</sup> N HCl. Zn concentration-response curves were obtained using tricine buffered Zn solutions (Paoletti *et al.*, 1997). Free Zn concentrations were calculated as in Fayyazuddin *et al.* (2000). For free Zn concentrations of 500 nM or more, the pH of the resulting solution was re-adjusted to pH 7.3 with NaOH. We did not account for the weak Zn chelating properties of solutions containing 100  $\mu$ M glutamate and glycine. However, when 10 mM glutamate and 100  $\mu$ M glycine was used, plotted free Zn concentrations were adjusted to take into account the additional buffering effect of glutamate. The dissociation constants for the reaction between Zn and glutamate used in Geochem were  $K_1 = 3.2 \times 10^{-7}$  M and  $K_2 = 3.2 \times 10^{-4}$  M (Martell and Smith, 1982). Note also that in solutions containing 10 mM glutamate and 1 mM Mg, Mg chelation by glutamate is negligible (Dawson *et al.*, 1986).

*Concentration-response curves.* For glutamate concentration-response curves (CRCs), the first agonist application and every third application thereafter was of a standard calculated to lie at around the EC<sub>30</sub> value. CRCs were conducted to either ascending or descending protocols and currents for individual cells plotted relative to their internal standards. For Zn and ifenprodil CRCs, the agonist solution was first applied to the oocyte to elicit a maximal current in the presence of Mg and once this current reached steady-state, Zn or ifenprodil was washed in, and inhibition judged relative to the preceding agonist induced current.

Glutamate CRCs were plotted for individual cells and fit with either single- or multiple-component Hill equations using CVFIT (from D. Colquhoun, UCL, London, UK). Individual curves were then normalized to their fitted maxima, pooled and re-fit with the appropriate Hill equation. In most cases curves were fitted free, with the exception of T690I and T690L, for which only the very base of the CRC could be estimated which were fit with their Hill slopes fixed to 1. Zn and ifenprodil CRCs were similarly fit with single- or multiple-component Hill equations using CVFIT. However, since inhibition was directly calculated as a percentage decrease in current, data from individual cells could be pooled before fitting. Note that for NR1/2A wt receptors only data up to 1  $\mu$ M were used for the fit. For Zn CRCs on NR1/2A<sub>H128SN614K</sub>, NR1/2A/2A<sub>H128SN614KT690I</sub> and NR1/2A<sub>N614KT690I</sub>/2C receptors, the maximum inhibition was arbitrarily fixed to 80%, the value obtained from free fits to NR1/2A wt receptors. This assumption will only affect the second low-affinity component of the triheteromeric Zn CRCs which is not the focus of the present investigation. Note also that for the triheteromeric receptors, the Hill slopes of the two components were fixed to 1. The NR1/2A<sub>N614KT690I</sub>/2B triheteromeric data was fitted with either two or three component Hill equations, the maximum inhibition was left free and the Hill slopes were fitted either free or fixed to 1. Ifenprodil CRCs for NR1/2A<sub>N614KT690I</sub>/2B receptors, were fitted with maximum inhibition fixed at 96% and the Hill slopes for both components fixed to 1. In all cases error bars represent the standard errors.

*Current-voltage relationships.* Current-voltage curves were obtained using slow (2 s) voltage-ramps from -100 to +50 mV. Capacitive and leakage currents were recorded before and after agonist applications, averaged and subtracted from the glutamate induced current traces using Clampfit 9.0 (Axon Instruments).

*Macroscopic kinetics of ifenprodil inhibition.* Because the kinetics of ifenprodil inhibition are particularly slow and certainly much slower than the ~2 s solution exchange in our recording chamber (Perin-Dureau *et al.*, 2002), they can be estimated directly from the current relaxations at the onset and offset of ifenprodil applications. The data shown in Fig. 7 were estimated with the fitting procedure of Clampfit 9.0.

*Modelling inhibition via the NTDs.* Inhibition was modeled using SCALCS (from D. Colquhoun) on the basis that Zn is an agonist at the NTD, albeit an agonist which brings about a conformational change leading to downstream inhibition of the NMDA receptor. SCALCS is designed to model channel activation, whereas we are studying inhibition of the NMDA receptor channel. To accommodate this discrepancy, we assumed that the conformational changes at the level of the NTDs were directly related to degree of inhibition, in turn represented as activity at a "channel gate". The efficacy of inhibition was consequently modeled as gating efficacy. Accordingly, the maximal possible activation (for a channel with a given conductance), equivalent to 100% inhibition, can be determined by artificially raising E<sub>2</sub> to >10,000. Restricted access to the downstream inhibitory machinery in scheme 2, was modeled as a sub-conductance state, since it is conceptually equivalent to a restricted conformational change at the channel gate. We also assumed that the maximum inhibition was limited by the conformational changes occurring at the level of the NTDs and not by the sensitivity of the downstream inhibitory machinery. Finally, inhibition is assumed to be independent of glutamate binding. This simplification is justified in view of the fact that, at NR1/2A receptors, Zn inhibition is

roughly constant over a wide range of glutamate concentration ( $>EC_{50}$ , unpublished observations) and that the likely effector (protons) have been shown to inhibit NMDARs independently of the state of agonist ligation (Banke *et al.*, 2005). Parameters used were as follows: Scheme 1:  $k_+ = 1 \times 10^8 \text{ M}^{-1}\text{s}^{-1}$ ,  $k_- = 2.95 \text{ s}^{-1}$ ,  $\beta_1 = \beta_2 = 100 \text{ s}^{-1}$ ,  $\alpha_1 = 555 \text{ s}^{-1}$ ,  $\alpha_2 = 25 \text{ s}^{-1}$ . Scheme 2:  $k_+ = 1 \times 10^8 \text{ M}^{-1}\text{s}^{-1}$ ,  $k_- = 8 \text{ s}^{-1}$ ,  $\beta = 101.25 \text{ s}^{-1}$ ,  $\alpha = 15 \text{ s}^{-1}$ .

CVFIT, SCALCS can be obtained from <http://www.ucl.ac.uk/Pharmacology/dc.html>.

## REFERENCES

- Anson, L.C., Chen, P.E., Wyllie, D.J., Colquhoun, D., and Schoepfer, R. (1998). Identification of amino acid residues of the NR2A subunit that control glutamate potency in recombinant NR1/NR2A NMDA receptors. *J Neurosci* 18, 581-589.
- Anson, L.C., Schoepfer, R., Colquhoun, D., and Wyllie, D.J. (2000). Single-channel analysis of an NMDA receptor possessing a mutation in the region of the glutamate binding site. *J Physiol* 527 Pt 2, 225-237.
- Armstrong, N., and Gouaux, E. (2000). Mechanisms for activation and antagonism of an AMPA-sensitive glutamate receptor: crystal structures of the GluR2 ligand binding core. *Neuron* 28, 165-181.
- Ayalon, G., and Stern-Bach, Y. (2001). Functional assembly of AMPA and kainate receptors is mediated by several discrete protein-protein interactions. *Neuron* 31, 103-113.
- Banke, T.G., Dravid, S.M. and Traynelis, S.F. (2005). Protons trap NR1/NR2B receptors in a nonconducting state. *J Neurosci* 25, 42-51.
- Béhé, P., Stern, P., Wyllie, D.J., Nassar, M., Schoepfer, R., and Colquhoun, D. (1995). Determination of NMDA NR1 subunit copy number in recombinant NMDA receptors. *Proc R Soc Lond B Biol Sci* 262, 205-213.
- Benveniste, M., and Mayer, M.L. (1991). Kinetic analysis of antagonist action at N-methyl-D-aspartic acid receptors. Two binding sites each for glutamate and glycine. *Biophys J* 59, 560-573.
- Brickley, S.G., Misra, C., Mok, M.H., Mishina, M., and Cull-Candy, S.G. (2003). NR2B and NR2D subunits coassemble in cerebellar Golgi cells to form a distinct NMDA receptor subtype restricted to extrasynaptic sites. *J Neurosci* 23, 4958-4966.
- Cathala, L., Misra, C., and Cull-Candy, S. (2000). Developmental profile of the changing properties of NMDA receptors at cerebellar mossy fiber-granule cell synapses. *J Neurosci* 20, 5899-5905.
- Chazot, P.L., Coleman, S.K., Cik, M., and Stephenson, F.A. (1994). Molecular characterization of N-methyl-D-aspartate receptors expressed in mammalian cells yields evidence for the coexistence of three subunit types within a discrete receptor molecule. *J Biol Chem* 269, 24403-24409.
- Chazot, P.L., and Stephenson, F.A. (1997). Molecular dissection of native mammalian forebrain NMDA receptors containing the NR1 C2 exon: direct demonstration of NMDA receptors comprising NR1, NR2A, and NR2B subunits within the same complex. *J Neurochem* 69, 2138-2144.
- Chen, N., Moshaver, A., and Raymond, L.A. (1997). Differential sensitivity of recombinant N-methyl-D-aspartate receptor subtypes to zinc inhibition. *Mol Pharmacol* 51, 1015-1023.
- Choi, Y.B., and Lipton, S.A. (1999). Identification and mechanism of action of two histidines residues underlying high-affinity Zn<sup>2+</sup> inhibition of the NMDA receptor. *Neuron* 23, 171-180.
- Clements, J.D., and Westbrook, G.L. (1991). Activation kinetics reveal the number of glutamate and glycine binding sites on the N-methyl-D-aspartate receptor. *Neuron* 7, 605-613.
- Cull-Candy, S.G., Brickley, S., and Farrant, M. (2001). NMDA receptor subunits: diversity, development and disease. *Curr Opin Neurobiol* 11, 327-335.

- Dawson, R.M.C., Elliott, D.C., Elliott, W.H., and Jones, K.M. (1986). Data for Biochemical Research, 3rd edn (New York, Oxford Science).
- Didier, M., Xu, M., Berman, S.A., and Bursztajn, S. (1995). Differential expression and co-assembly of NMDA zeta 1 and epsilon subunits in the mouse cerebellum during postnatal development. *Neuroreport* 6, 2255-2259.
- Dingledine, R.J., Borges, K., Bowie, D., and Traynelis, S.F. (1999). The glutamate receptor ion channel. *Pharmacol Rev* 51, 1-61.
- Dunah, A.W., Luo, J., Wang, Y.H., Yasuda, R.P., and Wolfe, B.B. (1998). Subunit composition of N-methyl-D-aspartate receptors in the central nervous system that contain the NR2D subunit. *Mol Pharmacol* 53, 429-437.
- Fayyazuddin, A., Villaroel, A., Le Goff, A., Lerma, J., and Neyton, J. (2000). Four residues of the extracellular N-terminal domain of the NR2A subunit control high-affinity Zn<sup>2+</sup> binding to NMDA receptors. *Neuron* 25, 683-694.
- Furukawa, H., and Gouaux, E. (2003). Mechanisms of activation, inhibition and specificity: crystal structures of the NMDA receptor NR1 ligand-binding core. *Embo J* 22, 2873-2885.
- Hawkins, L.M., Chazot, P.L., and Stephenson, F.A. (1999). Biochemical evidence for the co-association of three N-methyl-D-aspartate (NMDA) R2 subunits in recombinant NMDA receptors. *J Biol Chem* 274, 27211-27218.
- Ishii, T., Moriyoshi, K., Sugihara, H., Sakurada, K., Kadotani, H., Yokoi, M., Akazawa, C., Shigemoto, R., Mizuno, N., Masu, M., and et al. (1993). Molecular characterization of the family of the N-methyl-D-aspartate receptor subunits. *J Biol Chem* 268, 2836-2843.
- Kemp, J.A., and McKernan, R.M. (2002). NMDA receptor pathway as drug targets. *Nat Neurosci* 5, 1039-1042.
- Kew, J.N., Richards, J.G., Mutel, V., and Kemp, J.A. (1998). Developmental changes in NMDA receptor glycine affinity and ifenprodil sensitivity reveal three distinct populations of NMDA receptors in individual rat cortical neurons. *J Neurosci* 18, 1935-1943.
- Kniazeff, J., Bessis, A.S., Maurel, D., Ansanay, H., Prezeau, L., and Pin, J.P. (2004). Closed state of both binding domains of homodimeric mGlu receptors is required for full activity. *Nat Struct Mol Biol* 11, 706-713.
- Kunishima, N., Shimada, Y., Tsuji, Y., Sato, T., Yamamoto, M., Kumasaka, T., Nakanishi, S., Jingami, H., and Morikawa, K. (2000). Structural basis of glutamate recognition by a dimeric metabotropic glutamate receptor. *Nature* 407, 971-977.
- Kuusinen, A., Abele, R., Madden, D.R., and Keinanen, K. (1999). Oligomerization and ligand-binding properties of the ectodomain of the alpha-amino-3-hydroxy-5-methyl-4-isoxazole propionic acid receptor subunit GluRD. *J Biol Chem* 274, 28937-28943.
- Laube, B., Kuhse, J., and Betz, H. (1998). Evidence for a tetrameric structure of recombinant NMDA receptors. *J Neurosci* 18, 2954-2961.
- Low, C.M., Zheng, F., Lyuboslavsky, P., and Traynelis, S.F. (2000). Molecular determinants of coordinated proton and zinc inhibition of N-methyl-D-aspartate receptors. *PNAS* 97, 11062-11067.

- Luo, J., Wang, Y., Yasuda, R.P., Dunah, A.W., and Wolfe, B.B. (1997). The majority of N-methyl-D-aspartate receptor complexes in adult rat cerebral cortex contain at least three different subunits (NR1/NR2A/NR2B). *Mol Pharmacol* 51, 79-86.
- Martell, A.E., and Smith, R.M. (1982). *Critical stability constants*, Vol volumes 1-6 ((New York: Plenum)).
- Masuko, T., Kashiwagi, K., Kuno, T., Nguyen, N.D., Pahk, A.J., Fukuchi, J., Igarashi, K., and Williams, K. (1999). A regulatory domain (R1-R2) in the amino terminus of the N-methyl-D-aspartate receptor: effects of spermine, protons, and ifenprodil, and structural similarity to bacterial leucine/isoleucine/valine binding protein. *Mol Pharmacol* 55, 957-969.
- Mayer, M.L., and Armstrong, N. (2004). Structure and function of glutamate receptor ion channels. *Annu Rev Physiol* 66, 161-181.
- Meddows, E., Le Bourdelles, B., Grimwood, S., Wafford, K., Sandhu, S., Whiting, P., and McIlhinney, R.A. (2001). Identification of molecular determinants that are important in the assembly of N-methyl-D-aspartate receptors. *J Biol Chem* 276, 18795-18803.
- Monyer, H., Burnashev, N., Laurie, D.J., Sakmann, B., and Seeburg, P.H. (1994). Developmental and regional expression in the rat brain and functional properties of four NMDA receptors. *Neuron* 12, 529-540.
- Mott, D.D., Doherty, J.J., Zhang, S., Washburn, M.S., Fendley, M.J., Lyuboslavsky, P., Traynelis, S.F., and Dingledine, R. (1998). Phenylethanolamines inhibit NMDA receptors by enhancing proton inhibition. *Nat Neurosci* 1, 659-667.
- Neugebauer, R., Betz, H., and Kuhse, J. (2003). Expression of a soluble glycine binding domain of the NMDA receptor in *Escherichia coli*. *Biochem Biophys Res Commun* 305, 476-483.
- Paoletti, P., Ascher, P., and Neyton, J. (1997). High-affinity zinc inhibition of NMDA NR1-NR2A receptors. *J Neurosci* 17, 5711-5725.
- Paoletti, P., Perin-Dureau, F., Fayyazuddin, A., Le Goff, A., Callebaut, I., and Neyton, J. (2000). Molecular organization of a zinc binding N-terminal modulatory domain in a NMDA receptor subunit. *Neuron* 28, 911-925.
- Perin-Dureau, F., Rachline, J., Neyton, J., and Paoletti, P. (2002). Mapping the binding site of the neuroprotectant ifenprodil on NMDA receptors. *J Neurosci* 22, 5955-5965.
- Pin, J.P., Galvez, T., and Prezeau, L. (2003). Evolution, structure, and activation mechanism of family 3/C G-protein-coupled receptors. *Pharmacol Ther* 98, 325-354.
- Rachline, J., Perin-Dureau, F., Le Goff, A., Neyton, J., and Paoletti, P. (2005). The micromolar zinc-binding domain on the NMDA receptor subunit NR2B. *J Neurosci* 25, 308-317.
- Schorge, S., and Colquhoun, D. (2003). Studies of NMDA receptor function and stoichiometry with truncated and tandem subunits. *J Neurosci* 23, 1151-1158.
- Sheng, M., Cummings, J., Roldan, L.A., Jan, Y.N., and Jan, L.Y. (1994). Changing subunit composition of heteromeric NMDA receptors during development of rat cortex. *Nature* 368, 144-147.
- Smart, T.G., Hosie, A.M., and Miller, P.S. (2004). Zn<sup>2+</sup> ions: modulators of excitatory and inhibitory synaptic activity. *Neuroscientist* 10, 432-442.

- Sun, Y., Olson, R., Horning, M., Armstrong, N., Mayer, M., and Gouaux, E. (2002). Mechanism of glutamate receptor desensitization. *Nature* 417, 245-253.
- Sundström, E., Whittemore, S., Mo, L.L., and Seiger, A. (1997). Analysis of NMDA receptors in the human spinal cord. *Exp Neurol* 148, 407-413.
- Tovar, K.R., and Westbrook, G.L. (1999). The incorporation of NMDA receptors with a distinct subunit composition at nascent hippocampal synapses in vitro. *J Neurosci* 19, 4180-4188.
- Wafford, K.A., Bain, C.J., Le Bourdelles, B., Whiting, P.J., and Kemp, J.A. (1993). Preferential co-assembly of recombinant NMDA receptors composed of three different subunits. *Neuroreport* 4, 1347-1349.
- Watanabe, M., Inoue, Y., Sakimura, K., and Mishina, M. (1992). Developmental changes in distribution of NMDA receptor channel subunit mRNAs. *Neuroreport* 3, 1138-1140.
- Williams, K. (1993). Ifenprodil discriminates subtypes of the N-methyl-D-aspartate receptor: selectivity and mechanisms at recombinant heteromeric receptors. *Mol Pharmacol* 44, 851-859.
- Williams, K. (1996). Separating dual effects of zinc at recombinant N-methyl-D-aspartate receptors. *Neurosci Lett* 215, 9-12.
- Wollmuth, L.P., Kuner, T., and Sakmann, B. (1998). Adjacent asparagines in the NR2-subunit of the NMDA receptor channel control the voltage-dependent block by extracellular  $Mg^{2+}$ . *J Physiol* 506, 13-32.

## FIGURE LEGENDS

### Figure 1: NR1/2A receptors with only one active NTD Zn binding site are Zn sensitive

Cartoons show schematic representation of NR2 subunit domains, from top: NTD (blue circle, **X** for H128S mutation), glutamate binding site (red square) and pore domain (single letter code of the residue at the QRN site, K represents the Mg insensitive mutant N614K). Left: NMDAR currents (-80 mV) in 100  $\mu$ M glutamate and glycine. Application bars indicate wash-in of 1 mM Mg and 200 nM Zn. Right: currents in response to voltage ramps (-100 to +50 mV) in 100  $\mu$ M glutamate and glycine (control), after wash-in of 1 mM Mg (+Mg) and after additional wash-in of 200 nM Zn (+Zn). **(A)** NR1/2A wt receptors are almost completely inhibited by Mg at -80 mV, thus masking any effect of Zn. Ramps show that high-affinity Zn inhibition becomes evident at more depolarized potentials where Mg block is relieved. **(B)** All-mutant NR1/2A<sub>H128SN614K</sub> receptors are barely affected by the application of Mg or Zn, either at -80 mV or during voltage ramps. **(C)** Currents resulting from co-expression of all three subunits are mixtures of NR1/2A wt, all-mutant NR1/2A<sub>H128SN614K</sub> and triheteromeric NR1/2A/2A<sub>H128SN614K</sub> receptors. At -80 mV, addition of 1 mM Mg fully inhibits the wt component (cf A). Additional application of Zn now produces further inhibition which can only arise from an effect on the NR1/2A/2A<sub>H128SN614K</sub> receptors.

### Figure 2: Mutations at NR2A<sub>T690</sub> affect glutamate sensitivity

**(A)** Glutamate concentration-response curves, at -80 mV (-60 mV for NR1/2A wt) obtained from oocytes expressing NR1 and NR2A subunits. Curves shown, in descending order of potency are: NR1/2A wt >> NR1/2A<sub>T690V</sub> > NR1/2A<sub>T690A</sub> >> NR1/2A<sub>T690I</sub>  $\approx$  NR1/2A<sub>T690L</sub>. Data are shown fitted with the Hill equation, normalized to the fitted maximum. Right hand panel shows close-up of concentration-response curves for NR1/2A<sub>T690I</sub> and NR1/2A<sub>T690L</sub> (note y-axis scaling). **(B)** Glutamate concentration-response curves for T690I containing mutant receptors. No obvious shift is seen between NR1/2A<sub>N614KT690I</sub> or NR1/2A<sub>H128SN614KT690I</sub> receptors and NR1/2A<sub>T690I</sub> receptors, indicating that the H128S and N614K mutations do not affect glutamate sensitivity. Data were fitted with the Hill equation ( $n_H$  fixed = 1) and shown plotted relative to the response at 1 mM glutamate. Note that the T690I mutation produces such a dramatic shift that we can only measure the foot of the concentration-response curve. Error bars represent standard errors.

### Figure 3: Inclusion of the NR2A<sub>T690I</sub> mutation permits pharmacological isolation of triheteromeric NMDA receptors

Cartoons show schematic representation of the three possible NR2 subunit combinations for cells injected with NR1, NR2A and NR2A<sub>H128SN614KT690I</sub> cDNAs. Notation is the same as in Fig. 1; the T690I mutation is denoted by an **X** in the glutamate binding domain. The lower panel shows glutamate concentration-response curves recorded at -80 mV from oocytes expressing NR1, NR2A and NR2A<sub>H128SN614KT690I</sub> subunits, recorded in the absence (solid squares) or presence (open diamonds) of 1 mM Mg. The data are fitted by a two component Hill equation and normalized to the fitted maximum. Error bars represent standard errors. In the absence of Mg two components are readily distinguished;

the first component has an affinity identical to that of NR1/2A wt receptors and the second has an affinity intermediate between wt and all-mutant (see Fig. 2) and corresponds to the triheteromeric NR1/2A/2A<sub>H128SN614KT690I</sub> receptors. In the presence of 1 mM Mg, the wt component is almost completely abolished leaving an almost pure triheteromeric receptor population.

**Figure 4: NR1/2A receptors with only one active NTD Zn binding site show nanomolar Zn sensitivity**

**(A)** Typical current traces recorded in an oocyte expressing NR1, NR2A and NR2A<sub>H128SN614KT690I</sub> subunits. Currents, at -80 mV, were elicited by application of 10 mM glutamate and 100  $\mu$ M glycine in a background of 1 mM Mg, to isolate triheteromeric NR1/2A/2A<sub>H128SN614KT690I</sub> receptors. Currents are shown normalized (pre-Zn). The initial current for this cell was 400 nA. **(B)** Concentration-response curves showing Zn inhibition for NR1/2A wt ( $\Delta$ ), NR1/2A/2A<sub>H128SN614KT690I</sub> ( $\blacksquare$ ) and NR1/2A<sub>H128SN614K</sub> ( $\diamond$ ) receptors recorded at -80 mV (-30 mV for NR1/2A wt) in the presence of 1 mM Mg, 100  $\mu$ M glycine and either 100  $\mu$ M (NR1/2A and NR1/2A<sub>H128SN614K</sub>) or 10 mM glutamate (NR1/2A/2A<sub>H128SN614KT690I</sub>). NR1/2A/2A<sub>H128SN614KT690I</sub> receptors show a biphasic inhibition, with the first component in the nM range, the extent of which (14%) is intermediate between that of NR1/2A wt and NR1/2A<sub>H128SN614K</sub> receptors. Data are shown fitted with one or two component Hill equations. Each point is the average response of between 3 and 14 cells. Error bars represent standard errors. Right-hand panel shows a close-up of the inhibition of triheteromeric receptors in the nM range. Fitted parameters were: NR1/2A,  $IC_{50} = 17.6 \pm 0.6$  nM,  $n_H = 1.06 \pm 0.04$ ; NR1/2A<sub>H128SN614K</sub>,  $IC_{50} = 9.0 \pm 1.0$   $\mu$ M,  $n_H = 0.99 \pm 0.13$ ; NR1/2A/2A<sub>H128SN614KT690I</sub>,  $IC_{50s} = 28.6 \pm 8.1$  nM and  $5.0 \pm 0.9$   $\mu$ M, relative areas  $17.7 \pm 0.2$  % and  $82.3 \pm 0.2$  %,  $n_{Hs}$  fixed = 1.

**Figure 5: NR1/2A/2C receptors are inhibited by nanomolar Zn**

**(A)** Typical current traces from an oocyte expressing NR1, NR2A<sub>N614KT690I</sub> and NR2C subunits. Currents, at -80 mV, were elicited by application of 10 mM glutamate and 100  $\mu$ M glycine in a background of 1 mM Mg, to isolate triheteromeric NR1/2A<sub>N614KT690I</sub>/2C receptors. Currents are shown normalized (pre-Zn). The initial current for this cell was 430 nA. **(B)** Concentration-response curves showing Zn inhibition for NR1/2A wt ( $\Delta$ ), NR1/2A<sub>N614KT690I</sub>/2C ( $\blacksquare$ ) and NR1/2C wt ( $\diamond$ ) receptors recorded at -80 mV for triheteromeric receptors or -30 mV for wt receptors in the presence of 1 mM Mg, 100  $\mu$ M glycine and either 100  $\mu$ M (NR1/2A and NR1/2C) or 10 mM glutamate (NR1/2A<sub>N614KT690I</sub>/2C). NR1/2A<sub>N614KT690I</sub>/2C receptors show a biphasic inhibition, with the first component in the nM range, reaching a plateau intermediate between that of NR1/2A and NR1/2C receptors. Data are shown fitted with one or two component Hill equations. Each point is the average response of between 3 and 4 cells. Error bars represent standard errors. The right-hand panel shows a close-up of the inhibition of triheteromeric receptors in the nM range. Fitted parameters were: NR1/2A, as Fig. 4; NR1/2C,  $IC_{50} = 15.1 \pm 0.9$   $\mu$ M,  $n_H = 0.93 \pm 0.05$ ; NR1/2A<sub>N614KT690I</sub>/2C  $IC_{50s} = 5.6 \pm 3.8$  nM and  $10.3 \pm 2.9$   $\mu$ M, relative areas  $28.7 \pm 5.0$  % and  $51.3 \pm 2.8$  %,  $n_{Hs}$  fixed = 1.

**Figure 6: NR1/2A/2B receptors are Zn and ifenprodil sensitive**

**(A)** Concentration-response curves showing Zn inhibition for NR1/2A wt ( $\diamond$ ), NR1/2A<sub>N614KT690I</sub>/2B ( $\blacksquare$ ) and NR1/2B wt ( $\nabla$ ) receptors recorded at either -80 mV (triheteromeric receptors) or -30 mV (wt receptors) in the presence of 1 mM Mg, 100  $\mu$ M glycine and either 100  $\mu$ M (NR1/2A and NR1/2B) or 10 mM glutamate (NR1/2A<sub>N614KT690I</sub>/2B). NR1/2A<sub>N614KT690I</sub>/2B receptors show a triphasic inhibition, with the first component in the low nM range, producing an inhibition intermediate between that of NR1/2A and NR1/2B receptors. Data are shown fitted with one or three component Hill equations. Each point is the average response of between 3 and 4 cells. The right-hand panel shows a close-up of the inhibition of triheteromeric receptors in the nM range. Fitted parameters were: NR1/2A, as Fig. 4; NR1/2B,  $IC_{50} = 0.84 \pm 0.03 \mu$ M,  $n_H = 0.85 \pm 0.03$ ; NR1/2A<sub>N614KT690I</sub>/2B  $IC_{50s} = 15.1 \pm 2.7$  nM,  $0.83 \pm 0.28 \mu$ M and  $3.9 \pm 0.4 \mu$ M, relative areas  $38.0 \pm 4.6 \%$ ,  $25.8 \pm 4.2 \%$  and  $19.7 \pm 5.1 \%$ ,  $n_{Hs} = 0.78 \pm 0.09$ ,  $0.89 \pm 0.25$  and  $1.64 \pm 0.43$ . **(B)** Left: low  $\mu$ M concentrations of ifenprodil produce a concentration dependent inhibition of NR1/2A<sub>N614KT690I</sub>/2B receptors. Currents are shown scaled to give the same response in the absence of ifenprodil. The initial current for this cell before ifenprodil application was 720 nA. Right: concentration-response curves showing ifenprodil inhibition for NR1/2B wt ( $\blacktriangledown$ , +1 mM Mg, -30 mV;  $\triangle$ , - Mg, -60 mV), NR1/2A<sub>N614KT690I</sub>/2B triheteromeric ( $\blacksquare$ , +1 mM Mg, -80 mV) and NR1/2A<sub>N614K</sub> ( $\diamond$ , +1 mM Mg, -80 mV) receptors. Glutamate was applied at 100  $\mu$ M (NR1/2A<sub>N614K</sub> and NR1/2B) or 10 mM (NR1/2A<sub>N614KT690I</sub>/2B). NR1/2A<sub>N614KT690I</sub>/2B receptors show a biphasic inhibition, with the first component in the low  $\mu$ M range, resulting in inhibition intermediate between that of NR1/2B and NR1/2A<sub>N614K</sub> receptors. Data are shown fitted with one or two component Hill equations. Each point is the average response of between 4 and 9 cells. Fitted parameters were: NR1/2A<sub>N614K</sub>,  $IC_{50} = 487 \pm 24 \mu$ M,  $n_H = 0.99 \pm 0.06$ ; NR1/2B,  $IC_{50} = 142 \pm 8$  nM,  $n_H = 1.0 \pm 0.03$ ; NR1/2A<sub>N614KT690I</sub>/2B  $IC_{50s} = 0.80 \pm 0.17 \mu$ M and  $161 \pm 24 \mu$ M, relative areas  $20.6 \pm 1.1 \%$  and  $75.3 \pm 1.3 \%$ ,  $n_{Hs}$  fixed = 1. **(C)** Inhibition by Zn and ifenprodil on NR1/2A<sub>N614KT690I</sub>/2B receptors are superadditive. Left: ifenprodil added to receptors already inhibited by Zn (black trace) produces an inhibition proportionally greater than when ifenprodil is applied alone (red trace, scaled accordingly, same oocyte). Right: black bars: average percentage inhibition by Zn (100 nM) applied alone or on a background of ifenprodil (3  $\mu$ M). Grey bars: inhibition by ifenprodil (3  $\mu$ M) alone or on a background of Zn (100 nM). Where both inhibitors are present, inhibition by the second inhibitor applied is calculated as the percentage inhibition of the residual current after application of the first inhibitor. Note that, no matter the order of application, inhibition by Zn or ifenprodil is greater in the presence of the complementary inhibitor. Error bars represent standard errors in all cases.

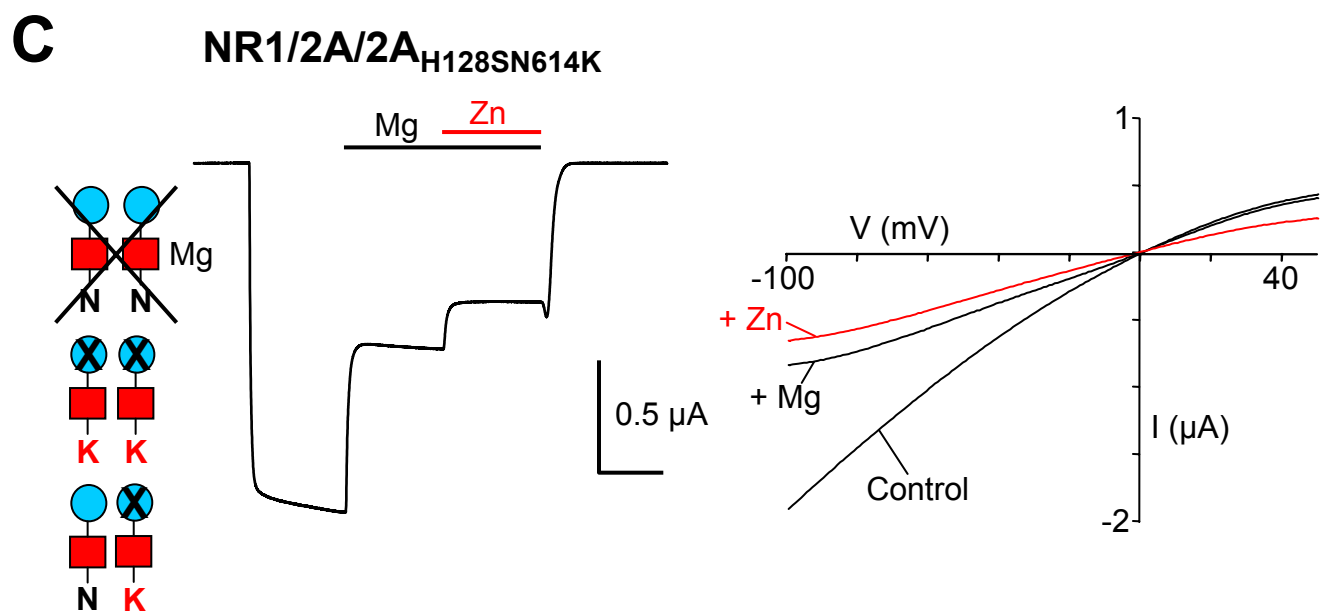
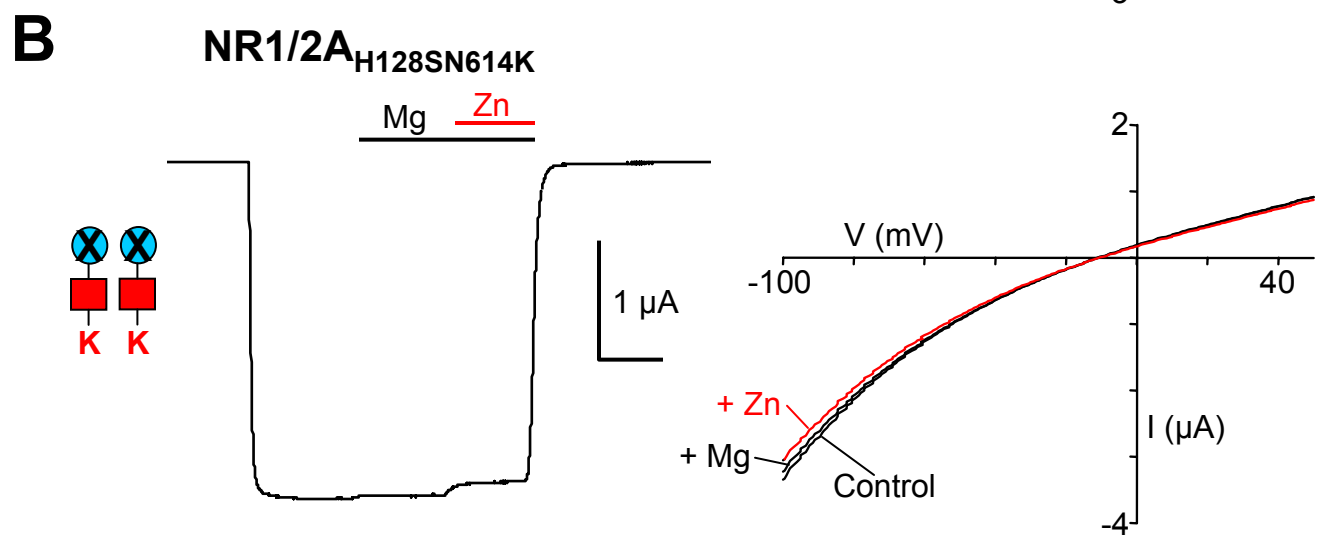
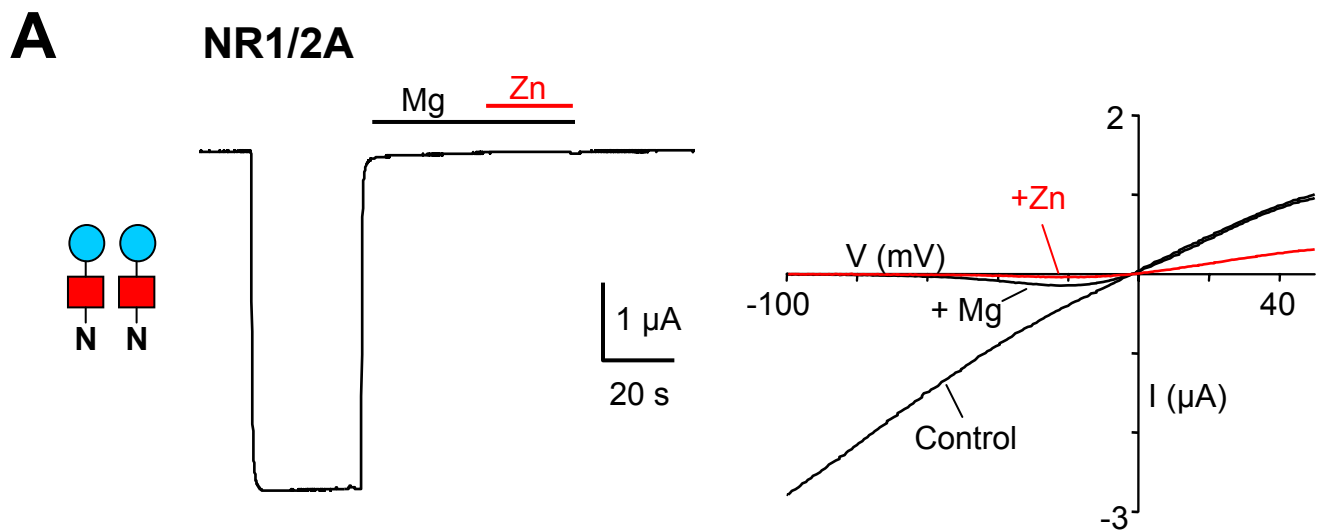
**Figure 7: Macroscopic kinetics of NR1/2A/2B triheteromeric and NR1/2B diheteromeric receptor inhibition by ifenprodil are distinct**

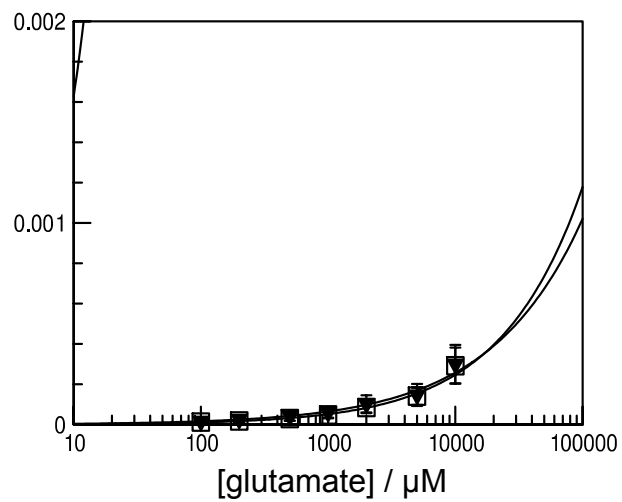
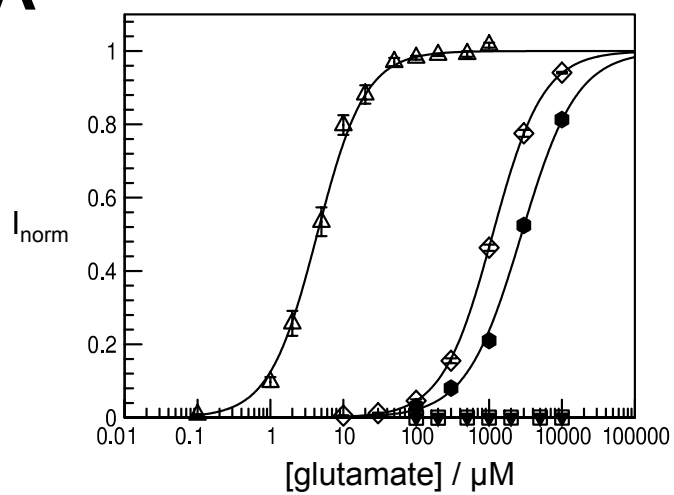
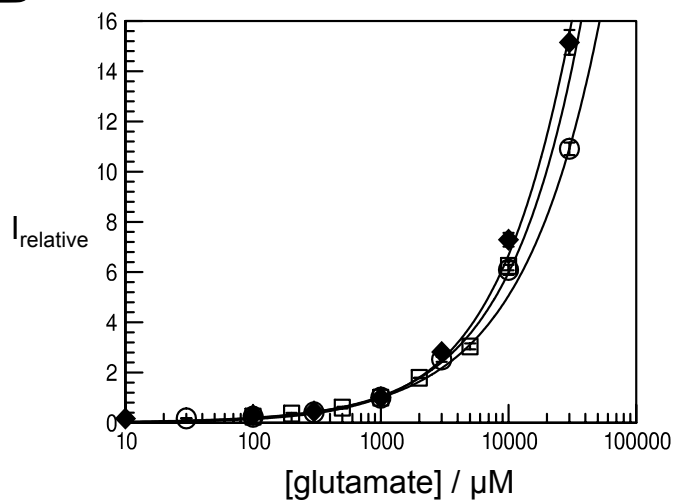
**(A)** Typical current traces recorded from oocytes expressing either NR1/2B wt (left) or NR1/2A<sub>N614KT690I</sub>/2B triheteromeric receptors (right). Currents were elicited on application of either 100  $\mu$ M (NR1/2B) or 10 mM (NR1/2A<sub>N614KT690I</sub>/2B) glutamate and 100  $\mu$ M glycine in a background of 1 mM Mg. Ifenprodil (3  $\mu$ M) was applied for the periods indicated by the application bars. Currents were recorded at either -30 mV (NR1/2B) or -80 mV (NR1/2A<sub>N614KT690I</sub>/2B). Note that NR1/2A<sub>N614KT690I</sub>/2B receptors are inhibited to a lesser extent than NR1/2B receptors. **(B)** Macroscopic on relaxations (left)

and off relaxations (right) for the traces shown in (A) (solid lines). Fits with single exponentials are superimposed on the experimental results (dashed grey lines). Traces are shown normalized to the same level of inhibition for comparison of kinetics. Note that the macroscopic on rate for triheteromeric receptors is slower than wt, whilst the macroscopic off rate is more rapid. **(C)** Scatter plot of time constants from fitted exponentials to macroscopic on rates ( $\tau_{on}$ ; left) and off rates ( $\tau_{off}$ ; right). Open circles show individual results,  $n=7$  and  $11$  for  $\tau_{on}$  and  $n=4$  and  $8$  for  $\tau_{off}$ , NR1/2B and NR1/2A<sub>N614KT690I</sub>/2B, respectively. Horizontal bar indicates mean of observations.

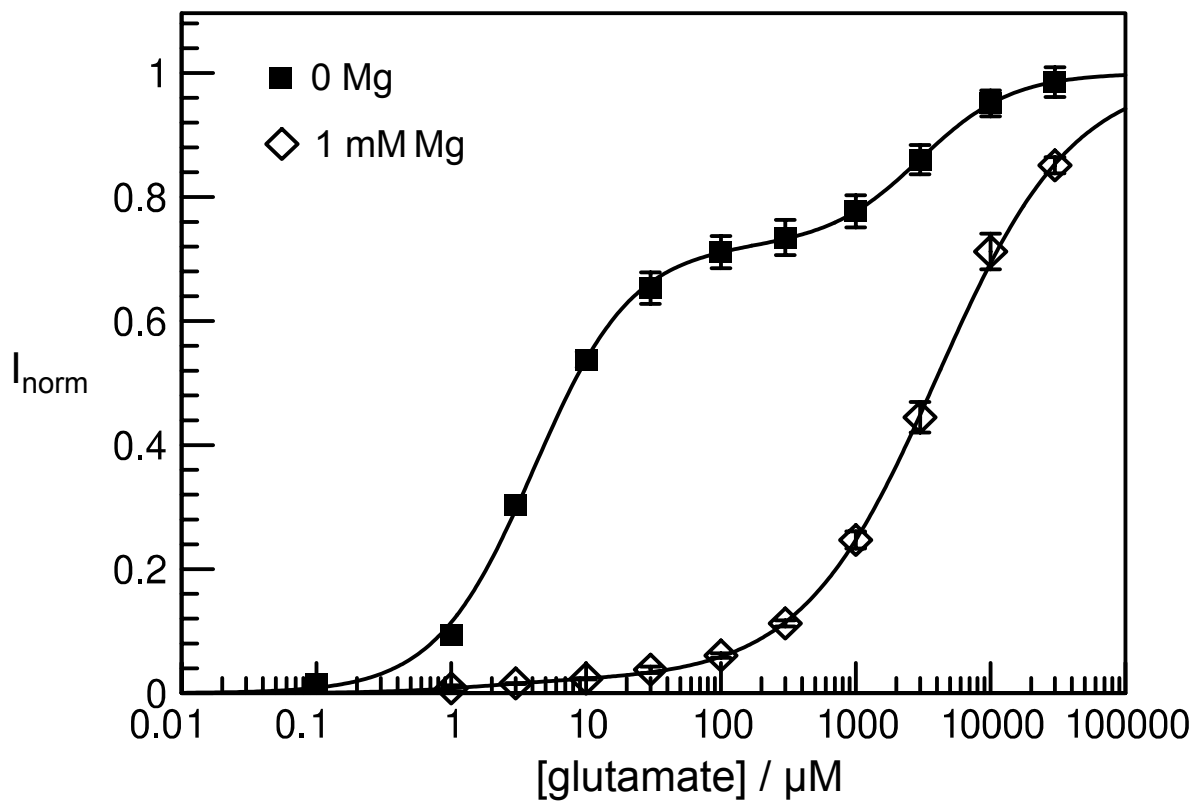
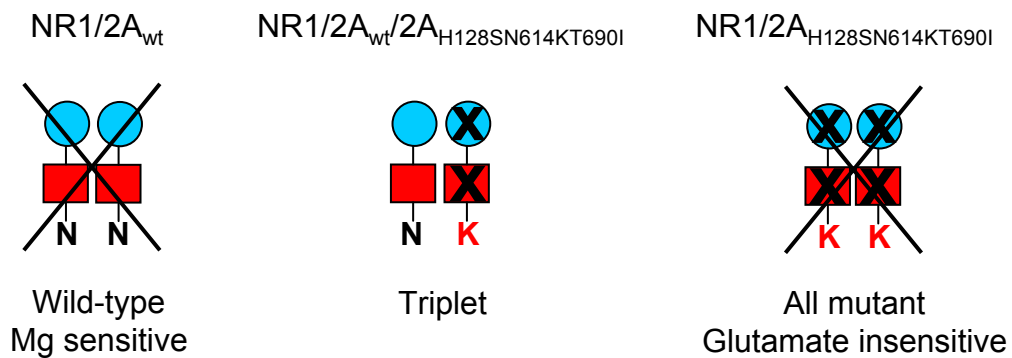
### Figure 8: Modelling inhibition of NMDA receptors via the NR2 NTDs

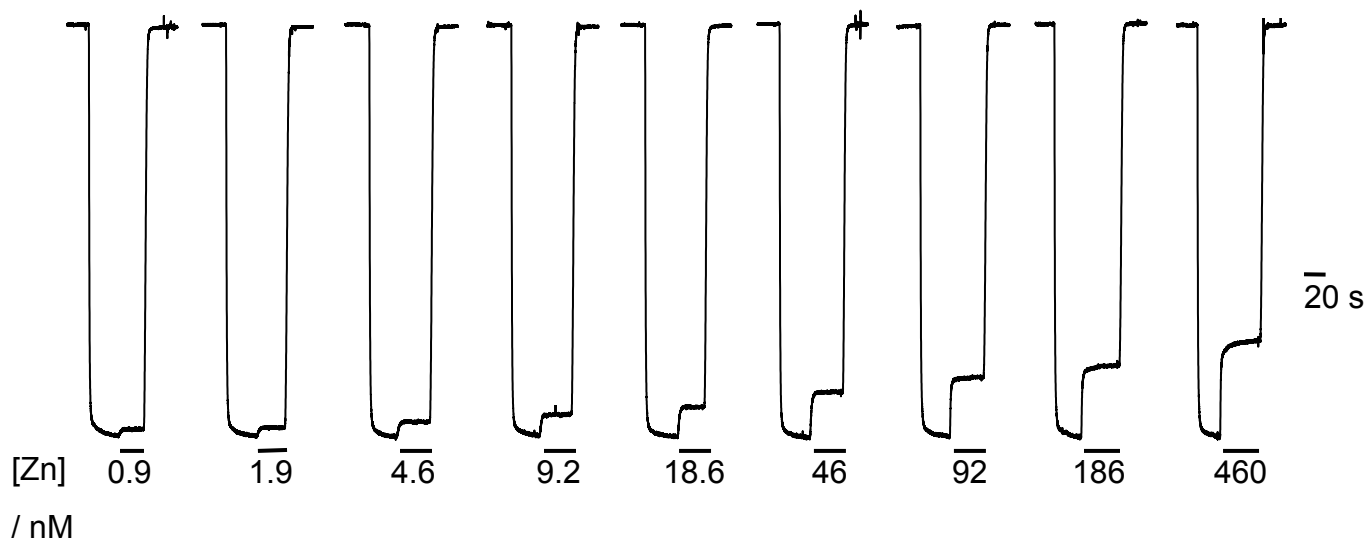
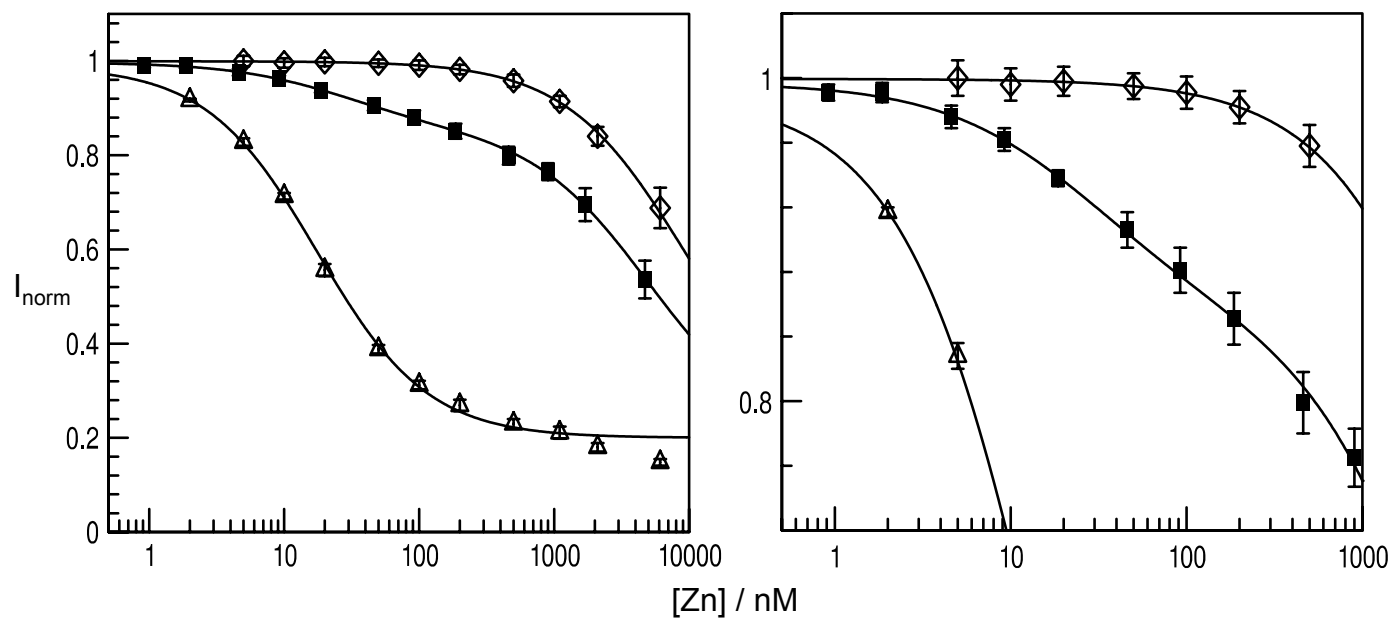
**(A)** Two possible reactions scheme for inhibition of NMDA receptors via the NR2-NTDs. Both schemes contain two binding steps because there are probably two NR2-NTDs per receptor. Because triheteromeric receptors with only one active site also show inhibition, we allow for inhibition from both singly- and doubly-liganded states. Scheme 1 (left) is based on the assumption that the NTDs can only move in a concerted manner, while Scheme 2 (right) is based on the alternative hypothesis, that the NR2-NTDs can move independently from one another. Paired blue pac-men represent the NR2-NTDs in either open (unbound, bound non-active) or closed (bound active) states. The light blue states are inactive (non-inhibiting), the dark blue states the active (inhibiting) states. Note that although the NR2-NTDs are represented as a dimer for simplicity, we do not know whether or not they are physically associated with one another in the intact receptor. **(B)** Theoretical Zn concentration-inhibition curves for three variations on the schemes shown in (A). Values for parameters were chosen to give the correct  $IC_{50}$  for wt receptors, the correct degree of inhibition for wt and triheteromeric receptors. The red lines (left and right) show the case of a triheteromeric receptor with only one active binding site (scheme 1, states R, AR and AR\*\*; scheme 2, states R, AR, AR\*). The blue lines show the case where inhibition arises only from the doubly-liganded, doubly-NTD-shut state (scheme 1, omission of the state AR\*\*; scheme 2 only A2R\*\* is inhibiting). The green lines (representing the wt scenario) are calculated on the basis of two sequential bindings with inhibition from both singly- and doubly-liganded receptors, thus giving access to all states. **(C)** Theoretical Hill slope-concentration curves for the corresponding concentration-inhibition curves shown in (B). Crosses indicate  $IC_{50}$  point for each curve. Note that allowing for singly-liganded inhibition results in a shallower Hill slope than when only doubly-liganded doubly-NTD shut receptors cause inhibition (blue versus green lines).

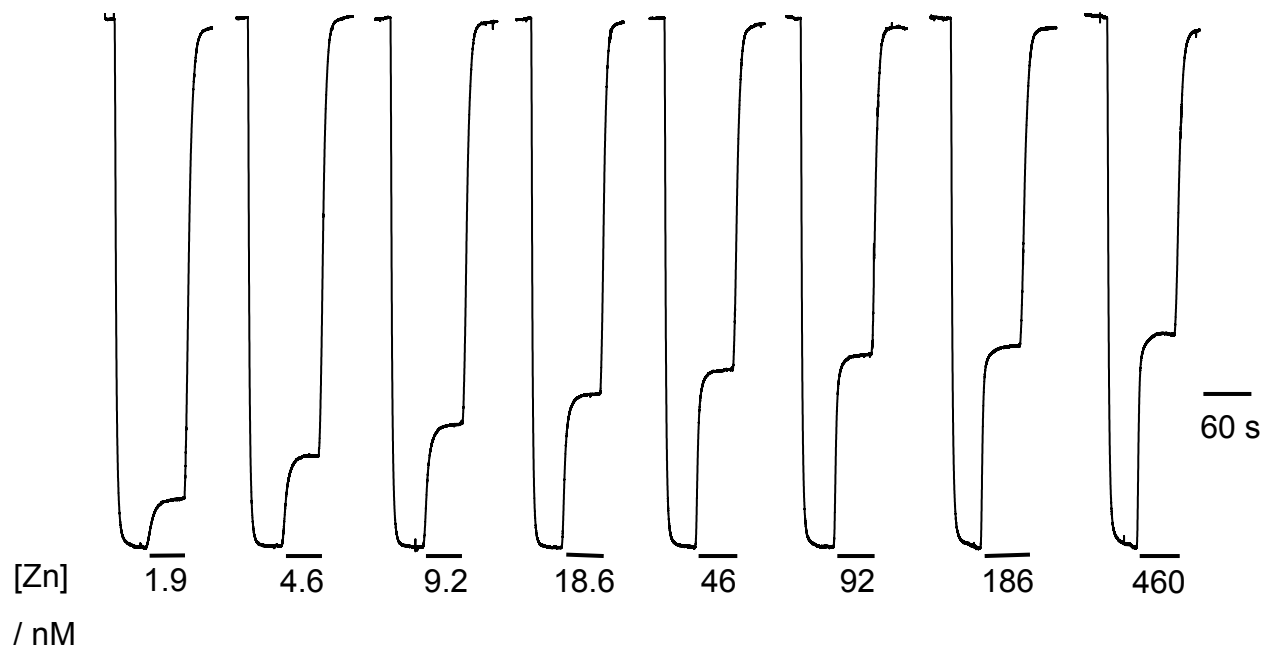
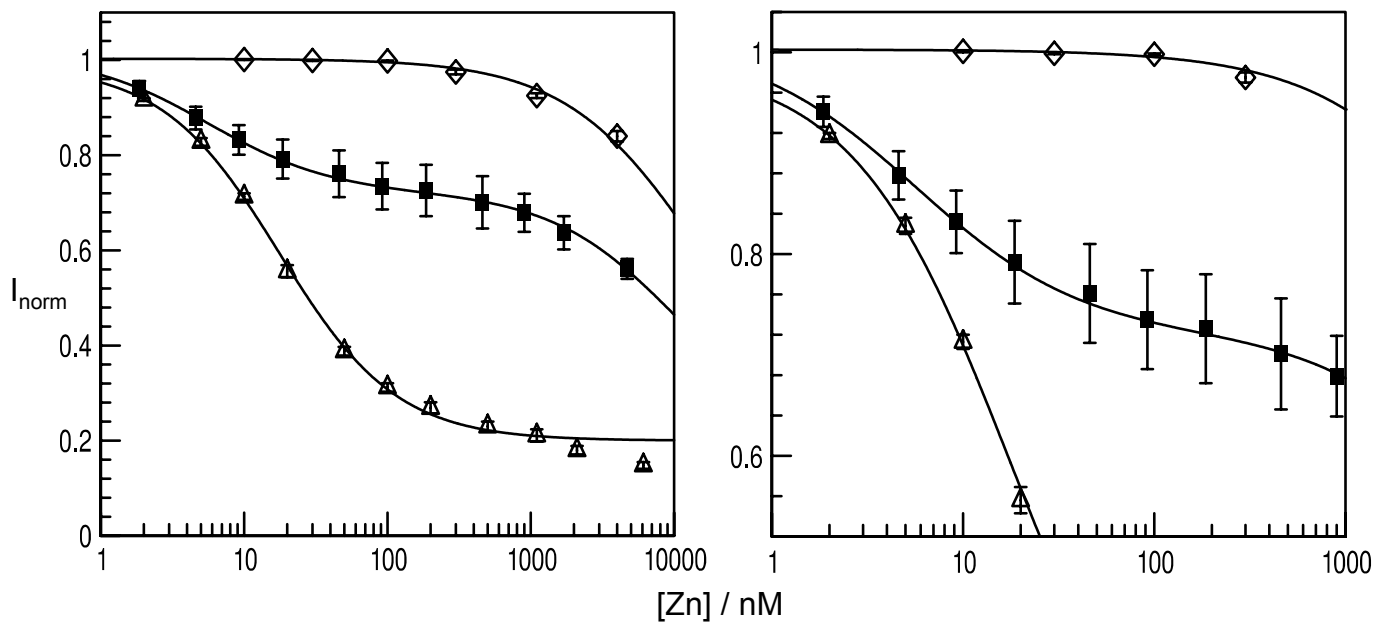


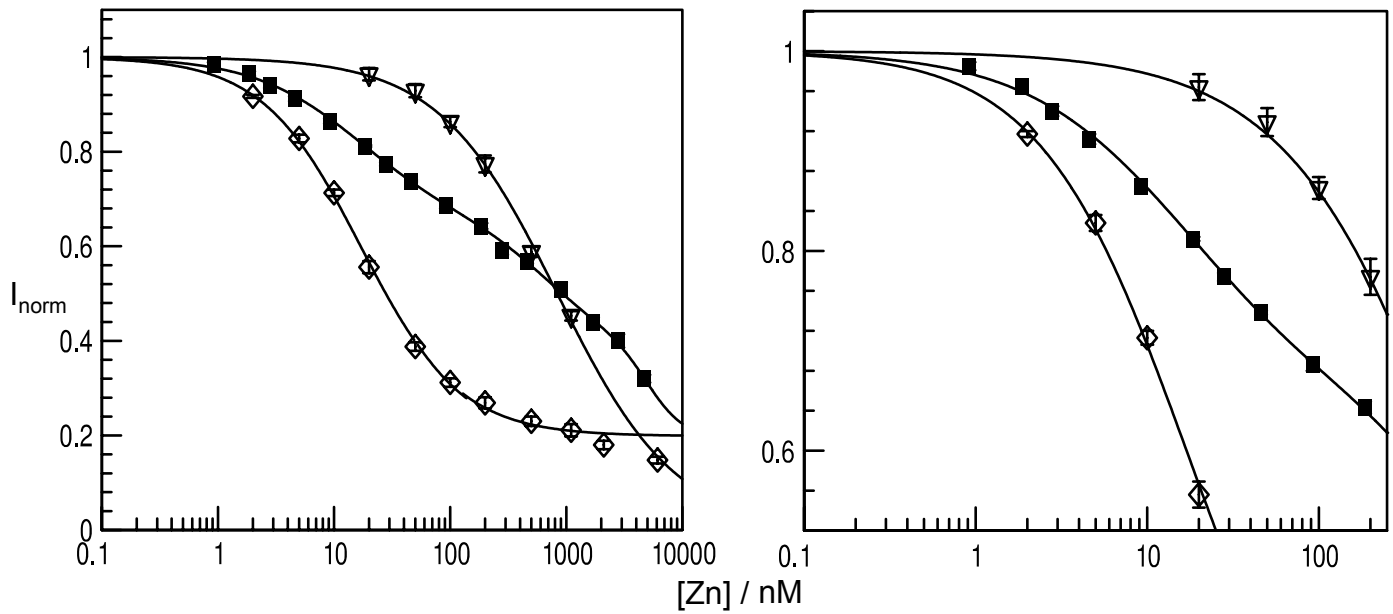
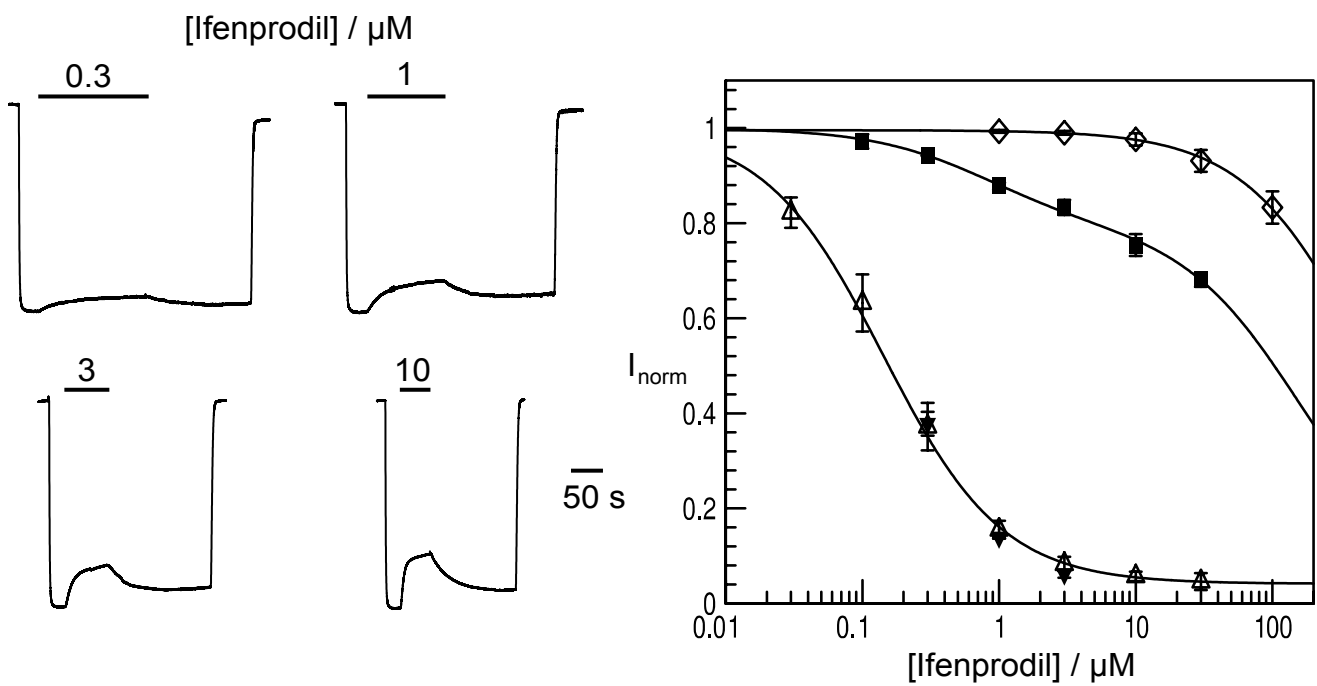
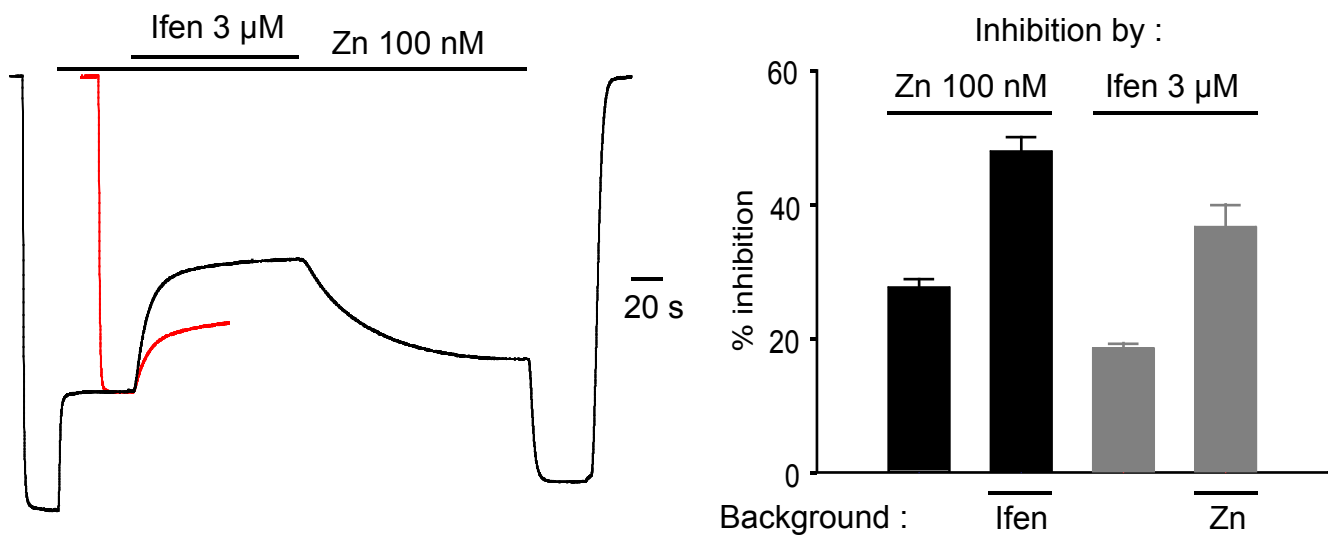
**A****B**

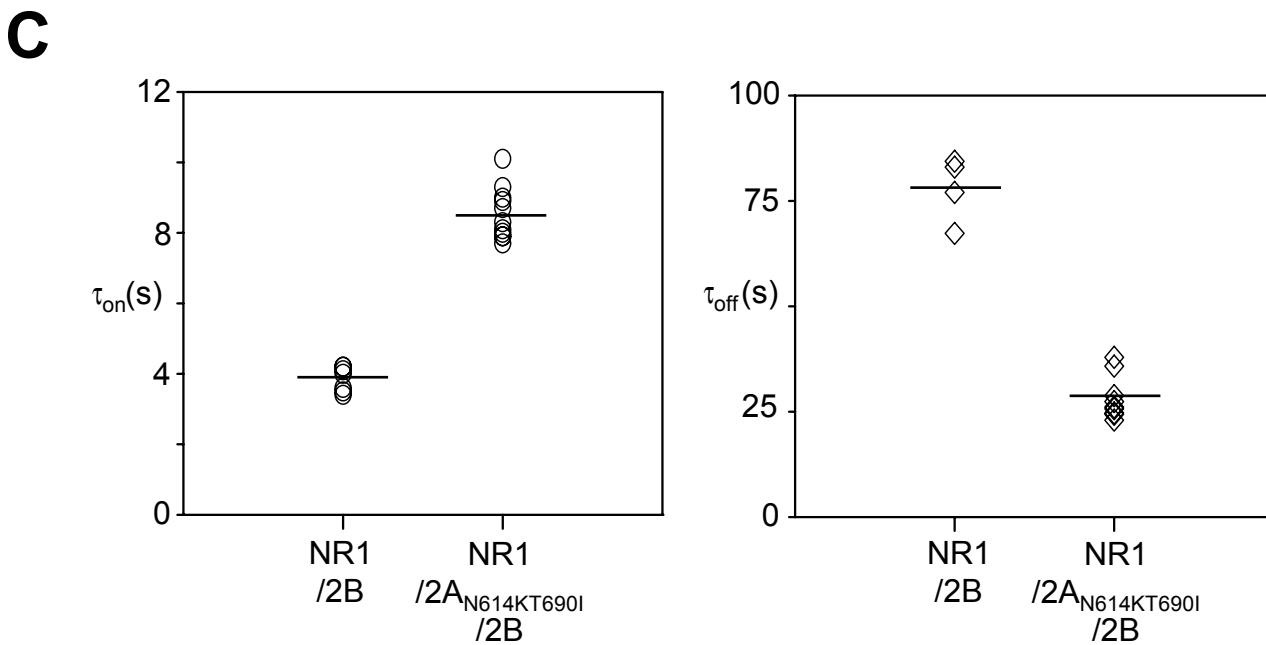
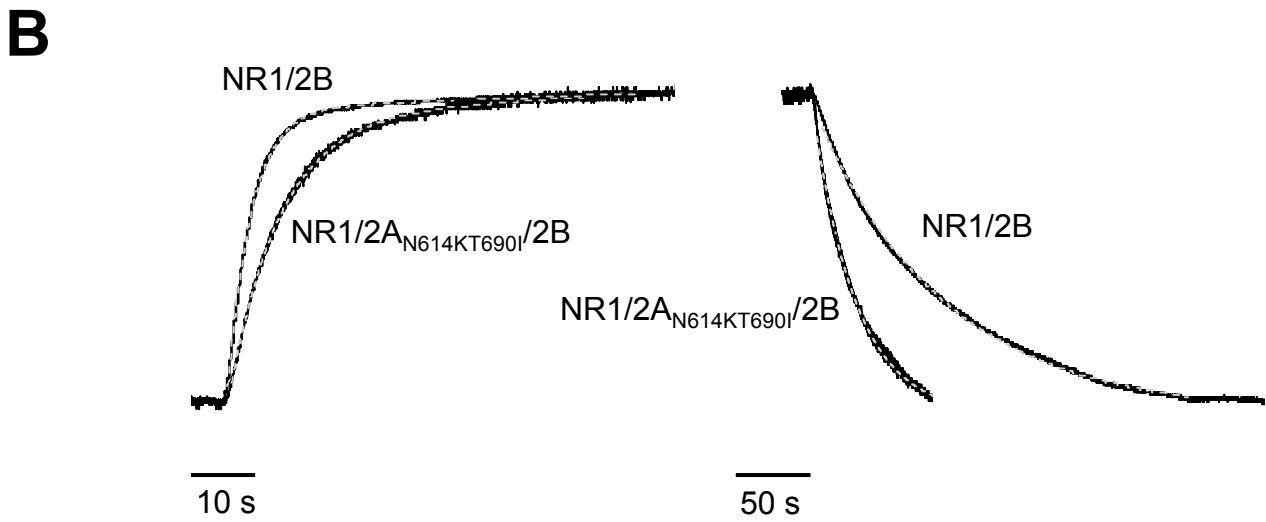
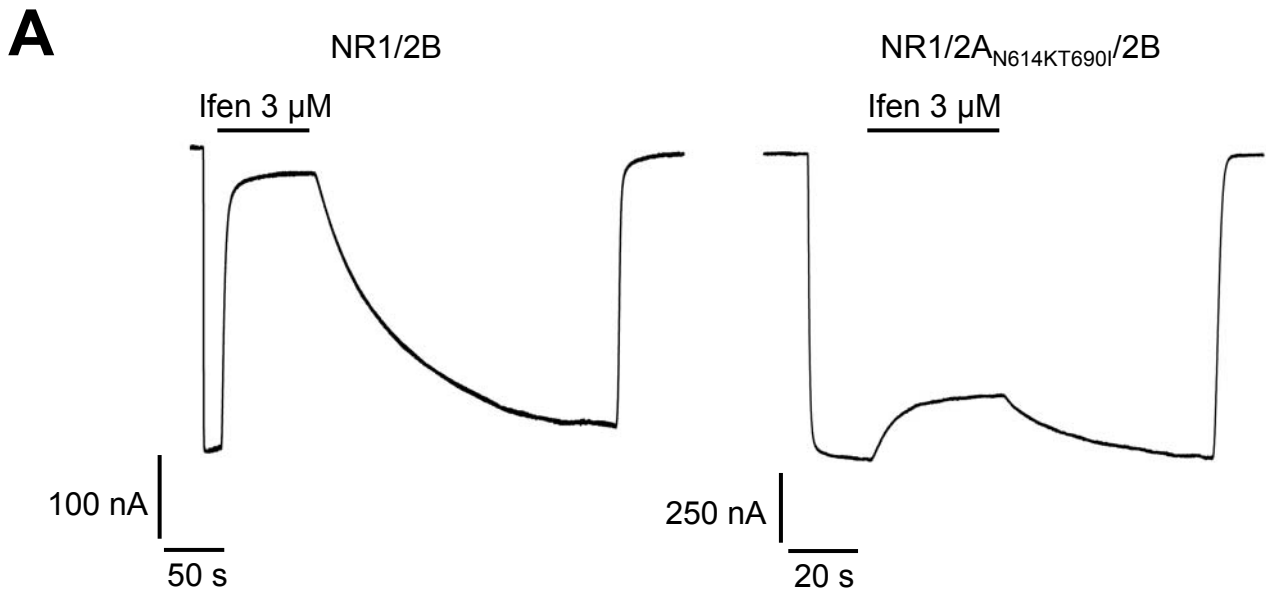
- $\triangle$  NR1/2A<sub>wt</sub>
- $\bullet$  NR1/2A<sub>T690A</sub>
- $\diamond$  NR1/2A<sub>T690V</sub>
- $\blacktriangledown$  NR1/2A<sub>T690L</sub>
- $\square$  NR1/2A<sub>T690I</sub>
- $\blacklozenge$  NR1/2A<sub>N614KT690I</sub>
- $\circ$  NR1/2A<sub>H128SN614KT690I</sub>

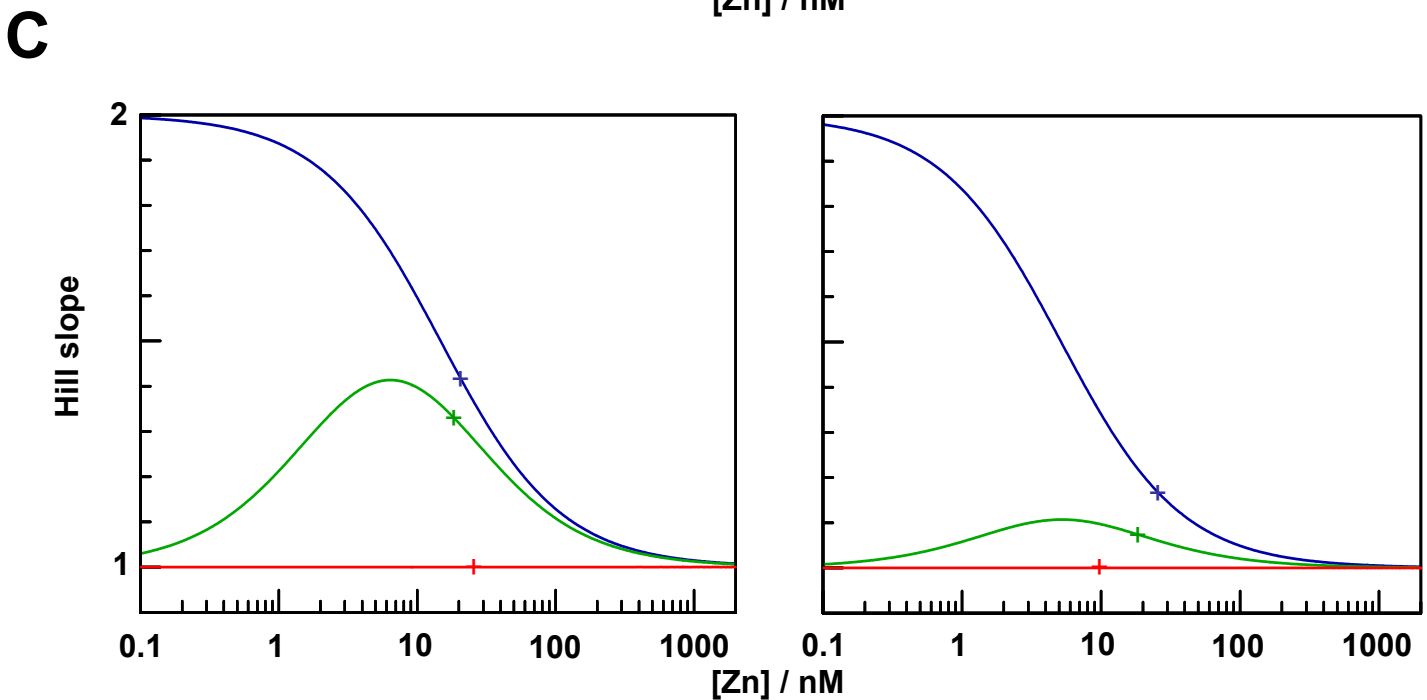
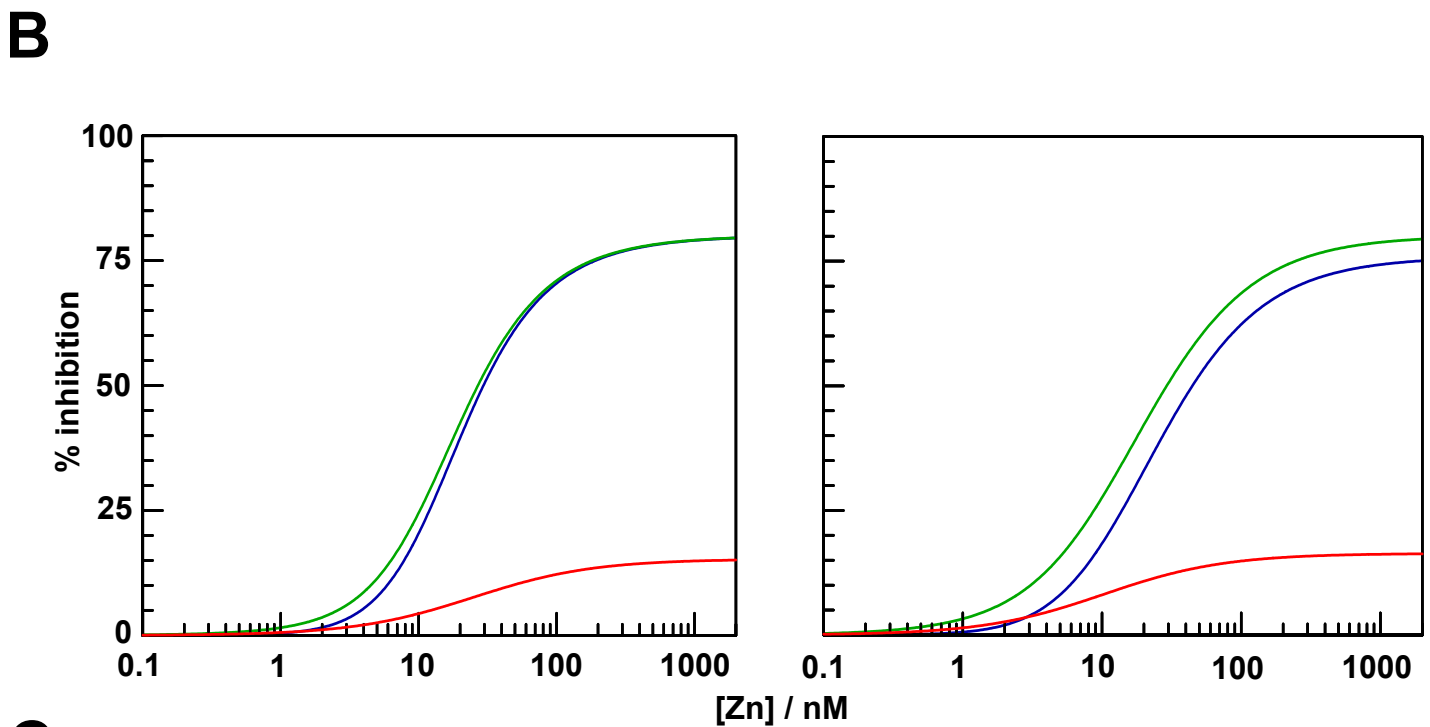
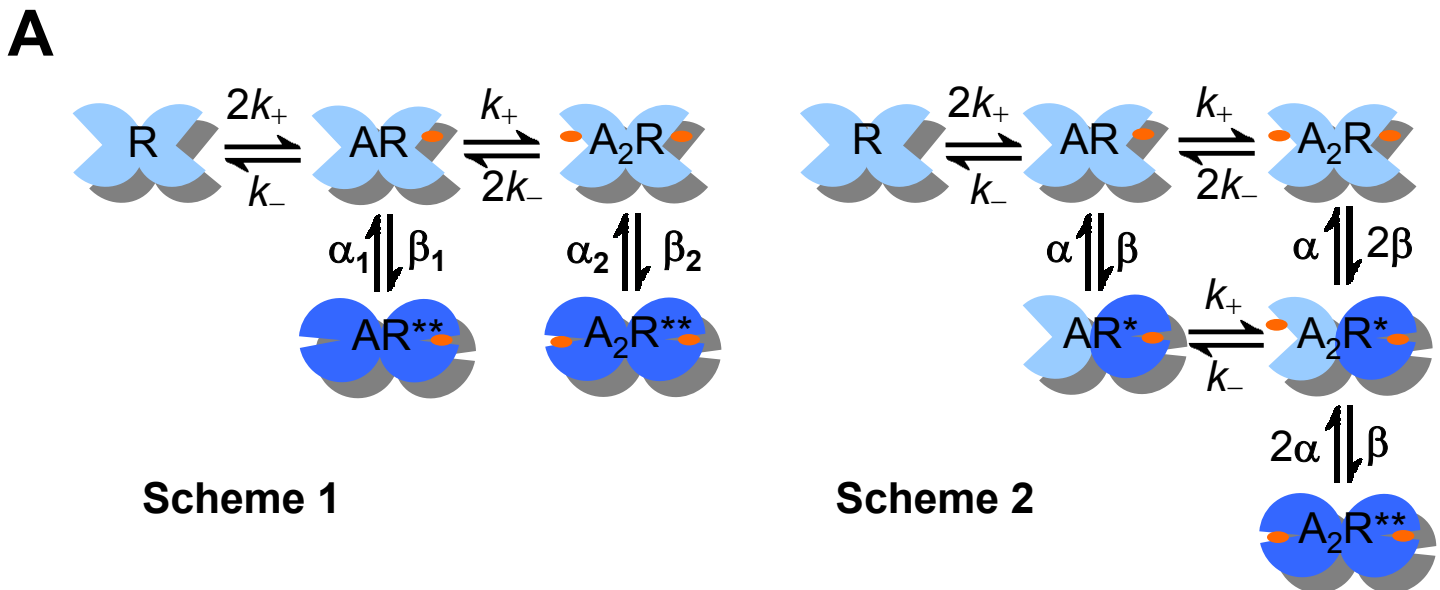


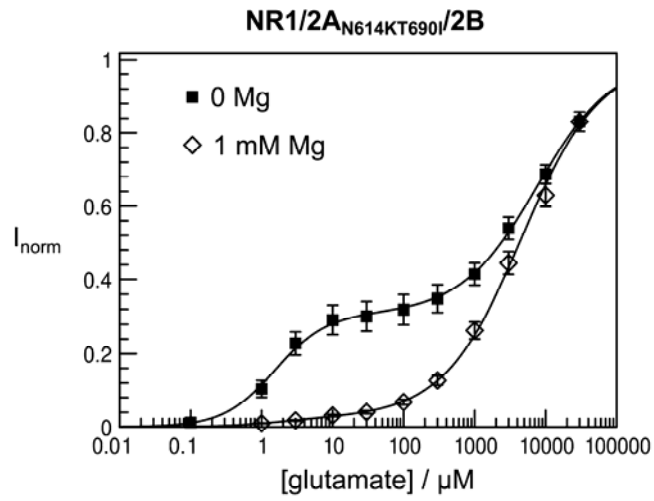
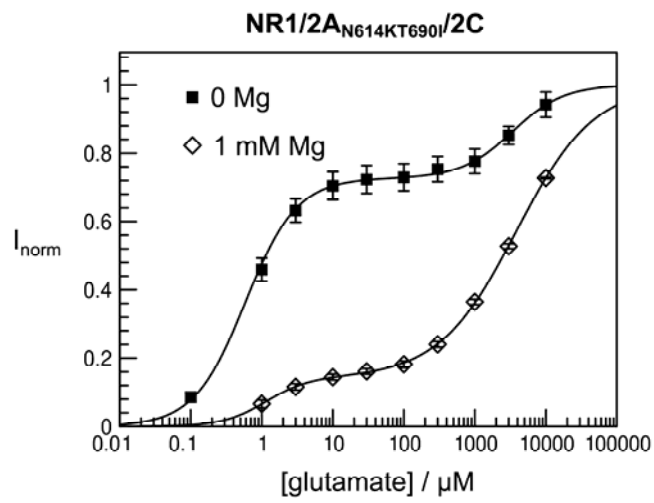
**A****B**

**A****B**

**A****B****C**

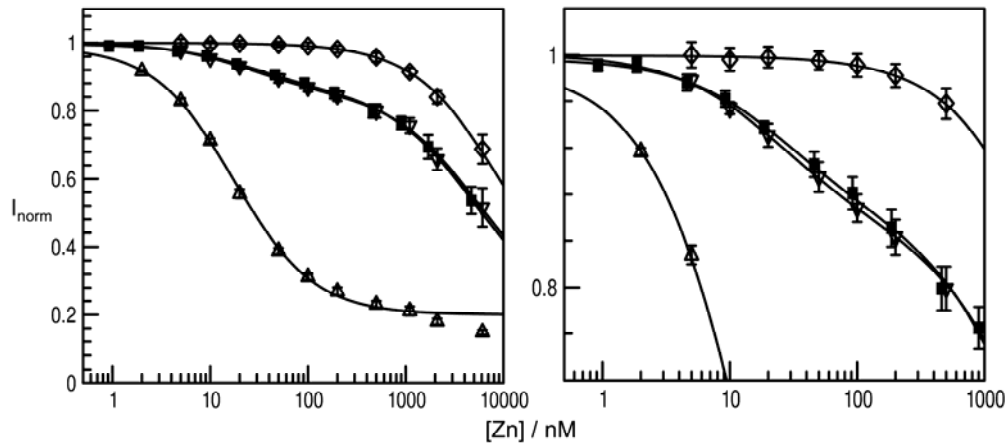




**A****B**

### Supplementary Figure 1: Pharmacological isolation of NR1/2A/2B and NR1/2A/2C triheteromeric NMDA receptors

**(A)** Glutamate concentration-response curves for oocytes expressing NR1, NR2A<sub>N614KT690I</sub> and NR2B subunits and recorded in the absence (solid squares) or presence (open diamonds) of 1 mM Mg. Each point shows the average response from 4-10 cells. In the absence of Mg two components are readily distinguished; the first component has an affinity identical to that of NR1/2B wt receptors ( $EC_{50} = 1.5 \pm 0.4 \mu\text{M}$ , relative area =  $30.7 \pm 0.3 \%$ ,  $n_H = 1.21 \pm 0.17$ ) while the second has an affinity intermediate between that of NR1/2B wt and all-mutant NR1/NR2A<sub>N614KT690I</sub> receptors (see Fig.2) and corresponds to the triheteromeric NR1/2A<sub>N614KT690I</sub>/2B receptors ( $EC_{50} \sim 7.5 \text{ mM}$ , relative area =  $69.3 \pm 15 \%$ ,  $n_H = 0.82 \pm 0.23$ ). In the presence of 1 mM Mg, the NR1/2B wt component is almost completely abolished (relative area =  $2.6 \pm 1.2 \%$ ) leaving an almost pure triheteromeric receptor population ( $EC_{50} = 4.6 \pm 1.9 \text{ mM}$ , relative area =  $97.4 \pm 12.7 \%$ ,  $n_H = 0.79 \pm 0.11$ ). **(B)** Glutamate concentration-response curves for oocytes expressing NR1, NR2A<sub>N614KT690I</sub> and NR2C subunits and recorded in the absence (solid squares) or presence (open diamonds) of 1 mM Mg. Data are from 3-12 cells. In the absence of Mg two components are readily distinguished; the first component has an affinity identical to that of NR1/2C wt receptors ( $EC_{50} = 0.6 \pm 0.1 \mu\text{M}$ , relative area =  $72.7 \pm 2.0 \%$ ,  $n_H = 1.12 \pm 0.1$ ) while the second has an affinity intermediate between that of NR1/2C wt and all-mutant NR1/NR2A<sub>N614KT690I</sub> receptors (see Fig.2) and corresponds to the triheteromeric NR1/2A<sub>N614KT690I</sub>/2C receptors ( $EC_{50} 3.4 \pm 2.3 \text{ mM}$ , relative area =  $27.3 \pm 8.1 \%$ ,  $n_H$  fixed = 1). In the presence of 1 mM Mg, the NR1/2C wt component is markedly reduced, but not completely abolished ( $EC_{50} = 1.1 \pm 0.2 \mu\text{M}$ , relative area =  $14.2 \pm 5.0 \%$ ,  $n_H = 1.44 \pm 0.44$ ). The majority of current in the presence of Mg is carried by the triheteromeric receptor population ( $EC_{50} = 3.8 \pm 0.5 \text{ mM}$ , relative area =  $85.8 \pm 8.3 \%$ ,  $n_H = 0.79 \pm 0.23$ ). Error bars represent standard errors.



**Supplementary Figure 2: The glutamate binding mutation NR2A<sub>T690I</sub> has little effect on Zn inhibition via the NR2-NTDs**

Shows data from Fig. 4B (see legend for details), with the Zn concentration-inhibition curve (in 1mM Mg at -80 mV) recorded from cells expressing NR1, NR2A and NR2A<sub>H128SN614K</sub> subunits superimposed ( $\nabla$ , n=13 cells). Under these recording conditions, approximately 90% of the current is carried by triheteromeric NR1/2A/2A<sub>H128SN614K</sub> receptors (see Results). Note that this curve is almost identical to that recorded from NR1/2A/2A<sub>H128SN614KT690I</sub> receptors ( $\blacksquare$ ) indicating that inclusion of the T690I glutamate binding mutation has little effect on Zn inhibition via the NR2A-NTD of the associated NR2A wt subunit. Right-hand panel shows a close-up of the inhibition of triheteromeric receptors in the nM range. Fitted parameters for  $\nabla$  were:  $IC_{50} = 25.0 \pm 4.6$  nM,  $5.6 \pm 1.0$   $\mu$ M, relative area  $19.0 \pm 1.4$  %,  $81.1 \pm 1.4$  %,  $n_H$  fixed = 1. Error bars represent standard errors.